A Review of Piezoelectric Fans for Low Energy Cooling of Power Electronics

Alastair Hales[a], Xi Jiang[a,*]

[a] *The School of Engineering and Materials Science, Queen Mary University London, Mile End Road, London, E1 4NS, UK*

Abstract

Power consumption from electrical devices increases year upon year, and as a result thermal management of power electronics is becoming ever more relevant. This review summarises the advancements made in the piezoelectric fan optimisation since their invention in the late 1970s. Energy consumption is highly relevant, and is an underlying theme throughout. Emphasis is placed on the methods undertaken to optimise designs for many different applications, and critical analysis of these processes is included. Comparison of data taken from different studies highlights the well-established rules of piezoelectric fan design and, more importantly for future advancements, also identifies the aspects of design which are not fully understood. Numerical modelling has become an essential tool for piezoelectric fan design optimisation since 2010, and the large majority of publications since have included computational methods to some degree. The optimisation of a single piezoelectric fan for a hot spot cooling application is well understood and, whilst always fundamental to the research field, does not pose the greatest potential for development in real life applications, as a single piezoelectric fan cannot replace a cooling system of any great size. Rather, the development of multiple fan arrays, which could ultimately replace alternative power electronic thermal management systems, should be strongly considered in the coming years.

*Corresponding author
Email address: xi.jiang@qmul.ac.uk (Xi Jiang)

Keywords: Low energy thermal management, Piezoelectric fan, Alternative air-mover, Design optimisation techniques, Numerical simulation, Validation

---

Contents

Nomenclature

A	Amplitude	m
A_{XC}	PE fan blade cross-sectional area	m^2
D_c	Driving coefficient	[dimensionless]
E	Young's modulus	$N.m^{-2}$
f	Frequency	Hz
f_r	Resonant frequency	Hz
g	Side wall gap	m
G	Empirical factor for plate bending theory	[dimensionless]
I	Second moment of area	m^4
K_{mag}	PE fan array apparent stiffness	m^{-3}
L	PE fan length	m
L_{FIN}	Heat sink fin length	m
L_{PZT}	PE actuator length	m
m	PE fan blade mass	kg
N	Number of PE fan blades in an array	[dimensionless]
P	Pitch between PE fans	m
S	Length of heated surface	m
t	Time	s
t_{BL}	PE fan blade thickness	m
W	PE fan blade width	m
W_{PZT}	PE actuator width	m
x	PE fan coverage of heated surface	m
y	PE fan blade displacement	m
Y	PE fan blade displacement at maximum amplitude	m
β	PE fan blade characteristic coefficient	$(kg.N^{-1}.m^{-3}.s^{-1})^{0.25}$
δ	Blade tip to heat source separation distance	m
ε	Blade tip extension beyond side wall	m
ρ	Density	$kg.m^{-3}$
σ	Poisson's ratio	[dimensionless]

1. Introduction

The cooling requirements of electronic systems call for new cooling technologies with low power consumption. Unlike traditional convection fans, piezoelectric (PE) fans are ultra-low power air movers, made up of a fan blade, a lead zirconate titanate (PZT) actuator and a clamp. In operation, a small amount of geometric expansion and contraction is generated in the actuator by an alternating electrical current. The actuator induces resonance in the blade, and the high oscillation amplitude and frequency disturbs the surrounding air sufficiently for vortex formation and to create significant downstream wind velocities. The basis of research in the field, therefore, is the optimisation of all aspects of a piezoelectric fan design to create maximum turbulence and vorticity, in the case of near field hot spot cooling, or maximum directional flow rate, in the case of bulk airflow generation.

PE fans were first considered at the end of the 1970s. Toda's publication [1] marks the beginning of PE fan development in the academic domain, whilst Kolm and Kolm were the first to patent a PE fan device, through *Piezo Electric Products Inc.* in 1985 [2]. Interest and research was driven by the need for a small, low power cooling device for use in electronic equipment, as other components shrank and assemblies became more compact. The original works are still very relevant, showing the field has undergone a process of continual optimisation, rather than a complete overhaul. This is testament to the quality of the original design.

Maaspuro published a review of the field in 2016 [3], which reported, in particular, on the design and construction of PE fans. These topics are covered, but this review will focus specifically on the potential for a reduction in the energy demanded by thermal management systems across the entire spectrum of power electronics. A thorough technical understanding is required to optimise PE fans, and the methods undertaken by researchers in the field to achieve this are analysed in detail.

It is evident that the demand for power electronics has outgrown advances

in thermal management systems in the last 30 years [4] [5]. In regard to energy consumption, the critical point has been reached where rapid innovation of air-moving technology is essential to avoid a slowing in the development and optimisation of power electronics. This is firstly due to the expansion of the industry sector: the worldwide electrical energy consumption increased three-fold between 2000 and 2010 [6] [7], and has continued to increase at the same rate since [8]. In certain technological fields, one third of this energy is being put towards cooling [9].

PE fans are very relevant for innovation in the immediate future, because of the complexity and economic cost of the current energy management solutions that implements liquid cooling or heat dissipation through phase change materials [5] [10] [11]. As a result, this technology is not widely implemented across a range of large industry areas, where air-cooling is heavily relied upon. For example, air-cooling is still used in 95% of computer technology worldwide [12]. Airflow is very often generated by axial fans which, amongst the other drawbacks considered in Section 6, demand a great deal of energy [13] [14]. At present, the PE fan is a viable alternative for certain applications involving moderate heat flux components [12], where they are easy to retrofit and provide comparable cooling capabilities for 50% of the power demand [15] [16] [17]. The challenge faced is the development of the technology to widen the field of possible applications, and this is a key theme throughout the review. There is great potential to dramatically reduce the worldwide energy consumption of thermal management systems with intelligent innovation in this field.

The demand for alternative air-moving technology has sparked an increase in published literature concerning PE fans in the last decade, and the considerable advancements in computational and numerical modelling over the same period has allowed researchers to understand the field in far more details than previously possible. This review will summarise such advancements and also expand on the areas which must still be investigated. The ratio of power consumed to heat transfer generated is an underlying theme throughout the review, as this will ultimately govern the degree of PE fan implementation in electrical

components in the coming years.

A single, simple PE fan can be seen as a clamped cantilever beam of uniform width, W, and thickness, t, being driven, typically from a power source of 1 - 10 mW, to oscillate at a certain frequency. The PE fan actuator is a strip of lead zirconate titanate (PZT). The blade is driven from the clamped end, and the strip most often covers its entire width. A typical PE actuator is 24mm to 35mm in length, covering 35% to 50% of the fan blade. The phenomenon of resonance is essential to the driving of a PE fan blade. The blade's fundamental resonant frequency, f_r, which is discussed in Section 3.1, must be matched by the AC power supplied to the actuator, in order to incite resonance in the blade. The result is an oscillation amplitude that can be thousands of times greater than the actual expansion and contraction induced in the actuator. Blades, typically, are 50 - 100 mm in length, and oscillate at 50 - 100 Hz to an amplitude of 1 - 15 mm.

In Section 2, the fundamental aspects of a single PE fan blade are set out. PE fan operational and geometric characteristics, and the results of blade confinement are covered in Section 3. The use of multiple blades is considered in Section 4, along with specific novel designs. In Section 5, the implementation and validation of numerical models is discussed. Finally, Section 6 discusses the potential energy saving benefits of PE fan technology in specific applications, and the competition to the technology in the present day.

2. Piezoelectric Fan Oscillation

It is essential to understand the fundamentals of piezoelectric fan design: variable parameters, blade motion characteristics and airflow generation. These principles are fundamental to the research field and will drive innovation. Figure 1 outlines the geometric and operational parameters of a single PE fan (Section 3) and a PE fan array (Section 4).

The mode shape of a PE fan, as it deflects, is theoretically defined by Equation 1 [18], where Y is the amplitude of deflection at any distance, x, along a

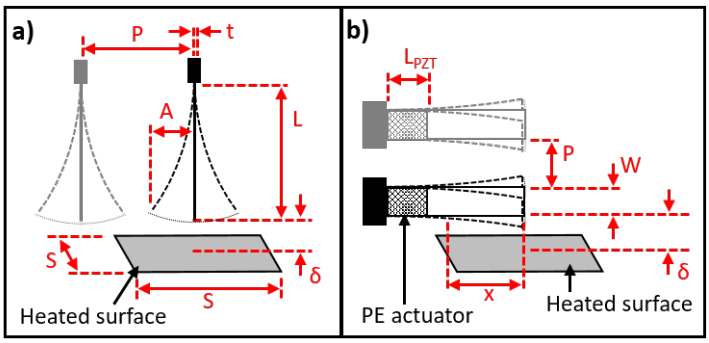

Figure 1: PE fan parameters and characteristics for (a) face-to-face and (b) edge-to-edge orientation

beam of length L. A_{XC}, the cross-sectional area of the blade. The coefficient β is defined in Equation 2 [18], where m, I and f_r are the mass, second moment of area and first resonant frequency of the blade, and E is the blade material's Young's modulus. In reality, the PZT actuator affects the blade shape, limiting the deflection in this region. Empirical functions have been defined in the literature to better describe Y, which are used in numerical models and discussed in Section 5.1.

$$Y(x) = A_{XC} \cdot \big[\big(sin(\beta \cdot L) - sinh(\beta \cdot L)\big) \cdot \big((sin(\beta \cdot x) - sinh(\beta \cdot x)\big) + \big(cos(\beta \cdot L) - cosh(\beta \cdot L)\big) \cdot \big((cos(\beta \cdot x) - cosh(\beta \cdot x)\big)\big] \tag{1}$$

$$\beta = \sqrt[4]{\frac{2\pi \cdot f_r \cdot m}{L \cdot I \cdot E}} \tag{2}$$

In motion, the displacement from the centre of oscillation, y, at any given time, t, along the PE fan blade is defined by Equation 3 [19]. Frequency, f, is defined by the frequency of the AC power input to the PE actuator, and is always set as the blade's the first resonant frequency, which is discussed in Section 3. The drive coefficient, D_c, defines the magnitude of power input, and is dimensionless for the purpose of describing PE fan blade motion in this case.

$$y(x,t) = D_c \cdot Y(x) \cdot sin(2\pi \cdot f \cdot t) \tag{3}$$

In unconfined conditions and in a domain of air, a vortex is formed from the blade during each sweep of the oscillation envolope. The majority of literature considers the 2D case, taken on a plane through the mid-point of the blade. The vortex rotates such that the air closest to the trailing edge of the blade has a positive downstream magnitude, as defined by Kolm and Kolm [2] in their original patent, and therefore two vortices are produced by the PE fan, rotating counter to one another, for each complete oscillation.

Vortex generation is shown in Figure 2 [20]. Formation initiation occurs at the blade tip close to peak amplitude ($\pi/2$) (2a) when its velocity is small and the static pressure difference from leading to trailing face is close to zero [20] [21]. Vortex growth occurs due to the pressure difference as the blade tip accelerates towards its oscillation centre (0) (2c) and until a phase of $-3\pi/11$ (2d) is reached [22]. Finally, the vortex detaches from the trailing edge as maximum amplitude is again reached ($-\pi/2$) (2e), when the blade tip has decelerated to a point that the pressure difference is once again close to zero. Vortices do not grow significantly as they propagate downstream [20]. However, the magnitude of the velocities surrounding a vortex reduce as propagation continues. The point at which the vortices can no longer be observed downstream has not been considered, but may provide useful analysis regarding the enhancement of turbulence, and therefore mass and heat transfer, at specified distances downstream from the blade tip.

Lin [23] reaches the same conclusions by considering the two air streams produced by the oscillating blade. A longitudinal impingement jet produced at the blade tip couples with the transversal air displacement driven by the movement of the blade face through a sweep, and results in the generation of the aforementioned vortex. Jeffers *et al.* [22] considered velocities on a different plane, at the blade tip but normal to the downstream directional vector (DDV). Phase locked PIV measurements at five points across a sweep of the oscillation envelope are shown in Figure 3. Edge effect significance was hypothesised by Bidakhvidi *et al.* [24], and is evident here. The acceleration from peak amplitude ($\pi/2$) (3a) to the oscillation centre (0) (3c) drives air around the edges of the

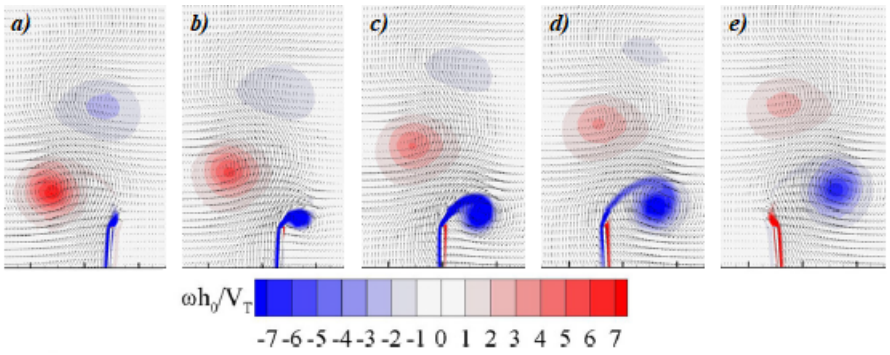

Figure 2: Instantaneous velocity fields and vorticity distribution through one sweep of the oscillation envelope, taken on a plane at the blade midpoint, at a) $\pi/2$, b) $3\pi/11$, c) 0, d) $-3\pi/11$ and e) $-\pi/2$ [20]

blade, from the leading to the trailing face. This process is still evident at $-3\pi/11$ (3d), but by the end of the sweep ($-\pi/2$) (3e), by which point the vortex has detached from the blade, airflow around the blade edges is minimal.

The airflow is driven by pressure difference, just as air moves around the blade tip [25]. The horseshoe shape of the air flow in this plane is typical of PE fan blade oscillation. When rupture of the vortices occurs, at the end of the sweep, edge vortices combine with the tip vortex, and form the basis of the generated downstream airflow [25].

It can be inferred from this discussion that blade width will have an effect on vortex generation, as the dominance ratio of the tip vortex to the edge vortices is altered. Whilst this parameter has been discussed in terms of downstream airflow and heat transfer enhancement (see Section 3), the effect on vortex generation is not yet fully understood [25].

3. Piezoelectric Fan Parameters and Characteristics

The geometric characteristics previously introduced (Figure 1) should be seen as the fundamental parameters, along with blade material properties, of a PE fan blade, as they govern the operational characteristics: frequency and amplitude. These intrinsic relationships will be evaluated in this section. Table

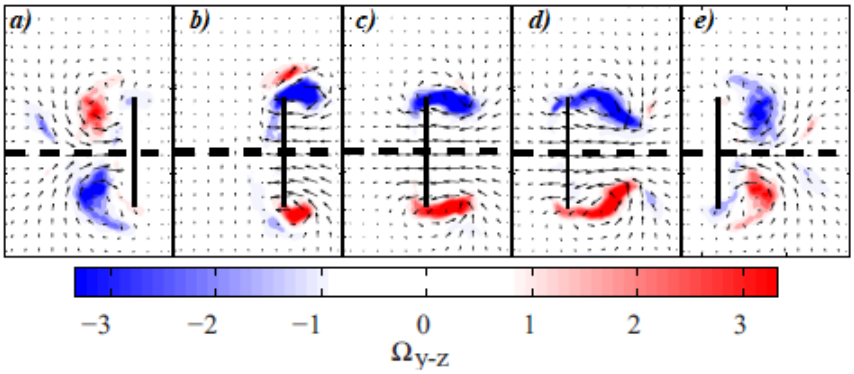

Figure 3: Instantaneous PIV imagery of velocity fields and vorticity distribution through one sweep of the oscillation envelope, taken on a plane normal to the DDV, at a) $\pi/2$, b) $3\pi/11$, c) 0, d) $-3\pi/11$ and e) $-\pi/2$ [22]

1 is included for reference. It becomes clear that both oscillation frequency and amplitude should be maximised for a typical application. Achieving this, however, is often difficult and compromise must be found.

Table 1: A summary of the reviewed PE fan properties and characteristics. NB: n/g: not given; PVC: polyvinyl chloride; PET: polyethylene terephthalate

	L/**mm**	W/**mm**	t_{BL}/**mm**	**Material**	L_{PZT}/**mm**	f_r/**Hz**	A/**mm**
[17]	64	12.7	n/g	Mylar	n/g	60	7.5
[23]	75	12.7	0.3	Polycarbonate	29	36.15	7.94
[26]	60.6-81	12-22	0.08-0.15	Brass/ Al/ Phos bronze	32-35	10-60	5.5
[27]	14.9-36.5	6.35-25.4	n/g	Mylar/ Stainless steel	n/g	61.7-256.2	2.5
[28]	76	12.7-25.4	0.2-0.5	PVC/ PET	29	23.2-53.9	6.35
[29]	68.5	12.7	0.27	Mylar	32	61	4
[30]	20	n/a (2D)	0.1	Red Copper	n/a (2D)	75	2.5
[31]	61-75	12-37	0.188-0.25	Mylar	n/g	28-53	3
[32]	50-63.5	10	0.076-0.13	Brass/ Stainless steel	n/g	20	15
[33]	47	12	0.4	Stainless steel	24	110	n/g
[34]	47	12	0.4	Stainless steel	24	110	4
[35]	47	12	0.4	Stainless steel	24	111	4.5
[36]	64	12.7	n/g	Mylar	n/g	60	6.35
[37]	47	12	0.4	Aluminium	n/g	115	n/g
[38]	68.5	12.7	0.27	Mylar	32	61	4
[39]	72	12.5	0.075	Stainless steel	24	110	6.25
[40]	64	12.7	n/g	Mylar	n/g	60	10
[41]	47	12	0.4	Stainless steel	24	111	5.01

3.1. Oscillation Frequency

Yoo *et al.* [26] define the resonant frequency of a PE fan blade, f_r, through Equation 4. Density (ρ), Poisson's ratio (σ) and Young's modulus (E) are

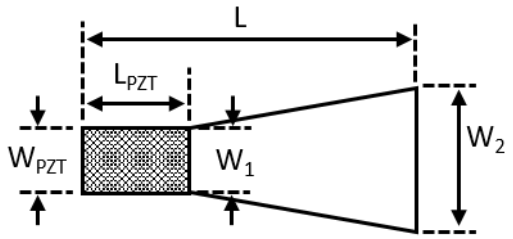

Figure 4: PE fan blade geometries varied by Lin *et al.*

material properties, and blade length (L) and thickness (t_{BL}) are geometric characteristics. G, a coefficient, is theoretically equal to 0.125π, but can be better defined experimentally in order to account for resistive effects on the motion. Blade width, therefore, is independent of frequency and this has been verified experimentally by Kimber and Garimella [27]. Blade width was varied in two otherwise identical PE fans by 400%. The respective blades' resonant frequencies varied by 0.6%.

$$f_r = G\frac{t}{L^2}\sqrt{\frac{E}{12\rho(1-\sigma^2)}} \tag{4}$$

Equation 4 assumes uniform blade width and thickness along its length, and as such the mass of the blade acts as a uniformly distributed load during forced vibration [42]. Lin *et al.* [28] consider the geometries summarised in Figure 4 and Table 2. Fan E is found to have the highest resonant frequency, and Fan D the lowest. When width ratio, W_2/W_1, is less than unity (*e.g.* Fan E), the mass of the blade creates an non-uniformly distributed load weighted towards the clamped end, and as such resonant frequency is increased [42] [18]. When width ratio is greater than unity (*e.g.* Fan D), the opposite occurs, and resonant frequency is reduced.

$$I = \frac{W \cdot t_{BL}^3}{12} \tag{5}$$

A blade's surroundings will also have a small effect on resonant frequency, due to the apparent mass increase caused by entrapped air [29]. This will be

Table 2: Dimensions of PE Fans used by Lin *et al.* [28]

PE Fan	L/ **mm**	L_{PZT}/ **mm**	W_{PZT}/ **mm**	W_1/ **mm**	W_2/ **mm**
A	76	29	12.7	12.7	12.7
B	76	29	12.7	19.1	19.1
C	76	29	12.7	25.4	25.4
D	76	29	12.7	12.7	25.4
E	76	29	12.7	25.4	12.7

discussed in Section 3.6.

Lin *et al.* [28] demonstrated that downstream airflow increases with oscillation frequency. A 17.3%, 36.7% and 47.7% increase in frequency induced a 22.4%, 49.3% and 97.0% increase in volume flow rate, respectively. A non-linear relationship between the two seems apparent, although further data is required to validate this hypothesis.

Wait *et al.* [43] considered higher modes of oscillation. Complex flow topologies are created which lead to greater mixing and cooling, but the drawbacks are more substantial. Damping losses and power consumption increase dramatically with higher modes, and airflow generation is reduced. Fairuz *et al.* [44] show, computationally, reduced vortex formation and a weaker downstream impingement jet with higher vibration modes. The average (maximum) heat transfer from a surface is reduced by 4% (7%) and 5% (9%) for the second and third modes respectively. Lei *et al.* [30] find the maximum heat transfer from a surface to be 15% greater in the first mode, compared to the second. Additionally, heat transfer performance is more volatile to orientation change away from the optimised state when oscillation is in the second mode.

3.2. Oscillation Amplitude

Table 1 shows amplitude (peak-to-centre) of the sampled PE fans is typically 10% of the PE fans total length, although this should not be seen as a rule which must govern all design: there is significant variance across the literature.

Oscillation amplitude is coupled to the geometry and material of the blade through Equations 1 and 2 but, crucially, can be varied independently through driving voltage adjustment [27]. Theoretically, driving voltage and vibration amplitude share a directly proportional relationship [45] [46]. In practice, damping on the blade, induced by the movement of air, becomes increasingly significant as driving voltage is increased [29] [45]. Given this, PE fan design should first consider the desired blade size and shape, and oscillation frequency: amplitude can be optimised subsequently without adversely effecting other characteristics.

Returning to blade shape considerations, Blade E required more power to achieve the same amplitude. This is also due to the distribution of the blade's mass as a load [18] [42].

Liu *et al.* [31] verified the logical hypothesis that heat transfer from a heated surface postioned in the generated airflow would increase with oscillation amplitude. Lin [23] reported the same findings, shown in Figure 5, and clearly separation distance does not affect this fundamental relationship.

Yoo *et al.* [26] found a direct relationship between amplitude and the generated non-directional air velocity, and the subsequent increased airflow and turbulence explains the aforementioned heat transfer enhancement. The non-directional element of this relationship is interesting to note, and at higher amplitudes, a blade may produce airflow across a broader spectrum of directions. Further work is required to investigate this hypothesis.

3.3. Piezoelectric Fan Geometric Characteristics

As discussed, the geometric characteristics of a PE fan define its operational characteristics. They also affect the generated airflow directly, and this design complication provides the basis for much of the optimisation across the literature.

Yoo *et al.* [26] demonstrated resonant frequency's $1/L^2$ relationship with blade length to a very high degree of accuracy in experimental work. Resultantly, PE fans are widely considered to be more effective at shorter lengths,

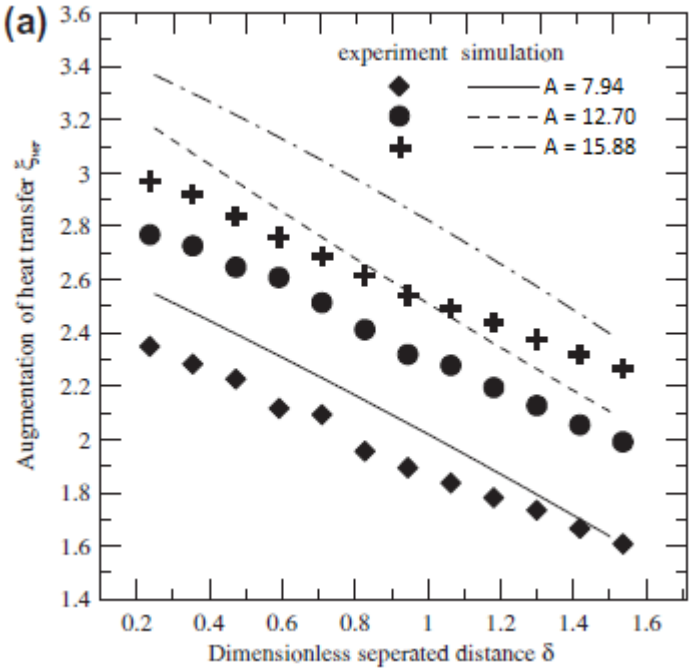

Figure 5: Dimensionless separated distance vs. heat transfer augmentation for different oscillation amplitudes [23]

where oscillation frequencies are significantly greater. Acikalin *et al.* [47] showed this benefit of shorter blades outweighed the increased volume of air displaced by a longer blade through each oscillation cycle. A trial of two blades, 76.2mm and 68.6mm in length, with respective oscillation frequencies of 62Hz and 103Hz, yielded a displaced air volume performance differential of 10-20% in favour of the latter.

However, there is not an established optimal blade length. This is beacuse the increased oscillation amplitude and blade surface area of longer blades are ideal for certain applications. In such cases blade thickness, which increases oscillation frequency in direct proportion, can be used to reduce the adverse effect. A simple experimental study considering two blades, differing in length by 3.17% [31], can be used to verify the theory. Theory states that this variance, alone, would reduce resonant frequency by 6.25%, but a 33.0% increase in blade

thickness to eventually increase frequency by 12.8%. The adverse effect is power demand which increases, as stipulated by Equation 5, at a cubic rate with thickness increase if oscillation amplitude is to be maintained.

In research, blade thickness is the most commonly used variable to adjust the resonant frequency of a blade, allowing for investigation across a range of frequencies. Unlike length, which would also alter frequency, the thickness of the blade has a negligable impact on the imparted air flow field [28].

Blade width is the least complex of the three length scale characteristics, as it is entirely independent of oscillation frequency and, through Equation 5, can be seen to increase power demand in proportion with itself as oscillation amplitude is maintained. Toda [1] hypothesised that blade width shared a proportional relationship with downstream airflow generation and a recent experimental study largely verifies this prediction [28]. Doubling width is shown to increase the average air velocity in the near and far field 110% and 105% respectively. The 10% and 5% error away from the original interpretation can be attributed to the blade edges, which are understood to dissipate some velocity away from the downstream direction and therefore are more influential for a blade of small width.

Width alteration effects become far more complex, and do affect both frequency and amplitude, when the width is not uniform along the blade length. Lin *et al.* [28] assessed the impact of non-uniform blade width on air propulsion and vortex generation, whilst maintaining oscillation frequencies and amplitudes through thickness adjustment. Results in Figure 6 show a stark difference in the vortex generation from Blade E compared to Blades A-D. Most streamlines behind the trailing face of the blade are dragged back to the trailing face during oscillation for Blades A-D, hence the generation of vortices. This is not the case for Blade E.

Downstream airflow generation from different blade shapes can be analysed from the experimental data plotted in Figure 7 [28]. Limits to the blade thickness range available meant Blades D and E are not directly compared. Comparison of the red ('Fan B, 37.3Hz' and 'Fan E, 37.2Hz') datasets, and also

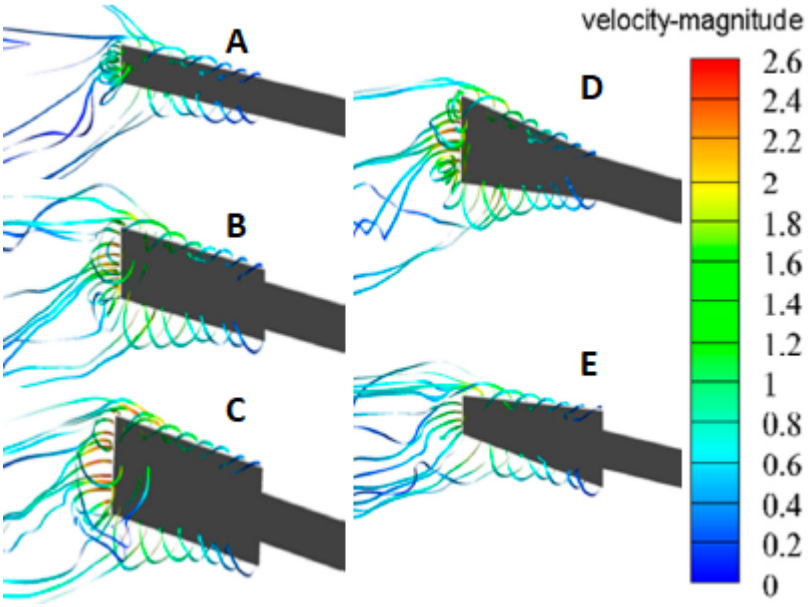

Figure 6: Streamlines leading to vortex generation from PE fan blades with unique geometric characteristics [28]

the black ('Fan B, 39.5Hz' and 'Fan E, 39.9Hz') datasets, shows inferior downstream air velocity is generated by a narrow tipped blade. Considering the blue ('Fan B, 31.3Hz' and 'Fan D, 31.1Hz') datasets, the wide tipped blade generated higher air velocities in the near vicinity, but performance diminishes more rapidly downstream. The superior near field velocities suggest greater turbulence close to the blade tip, and further work in the area could reveal additional benefits of altering the blade shape for some specific applications.

Material properties are also of importance for PE fan design optimisation and density, Young's modulus and Poisson's ratio can each be found in Equation 4 [26]. Shyu and Syu [48] found blade material to have a significant bearing on the performance of a PE fan operating within a finned heat sink, when power input was maintained. A mylar blade, E=2.28GPa, operates at a lower frequency (38.5Hz) but achieves significantly greater oscillation amplitude (10.4mm) than the aluminium alloy (70GPa, 75.5Hz, 4.5mm) or stainless steel (200GPa, 52.5Hz, 3mm) blades. Heat transfer was enhanced by 225% when the mylar blade was

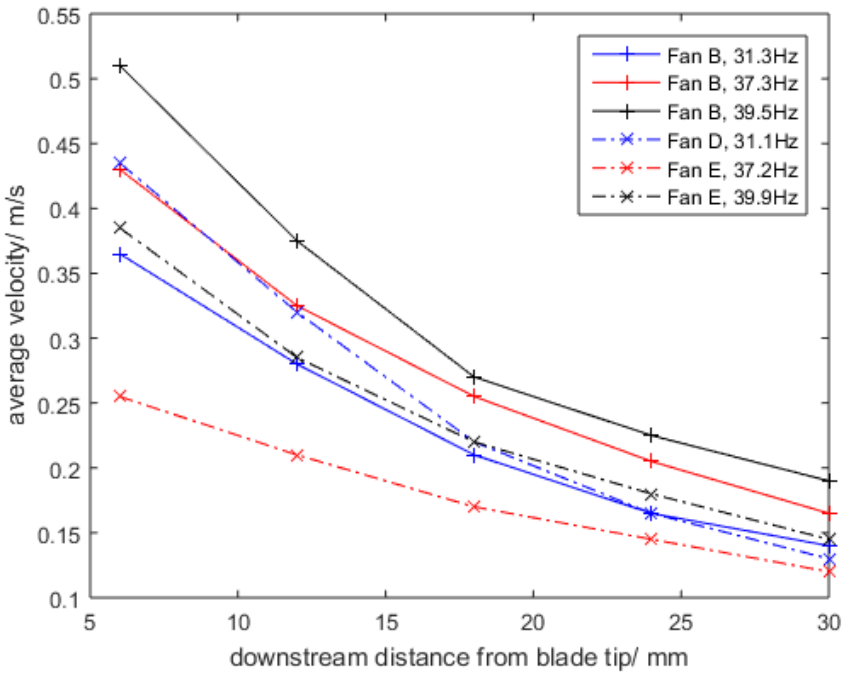

Figure 7: Air velocity at certain distances downstream for three unique blade shapes, oscillating at comparable frequencies [28]

used, but by just 105% and 60% for the aluminium and stainless steel blades respectively.

3.4. Piezoelectric Fan Orientation

The orientation of a PE fan to a heated surface has been considered widely. Several considerations must be made, as detailed below.

1. Is the heated surface in the horizontal or vertical plane?
2. Is the PE fan orientated horizontally or vertically (Figure 8a)? NB: For vertical orientation, all reviewed literature assumes the PE fan to be facing down.
3. For horizontal orientation, is the blade oscillating around a horizontal or vertical axis (Figure 8a)?

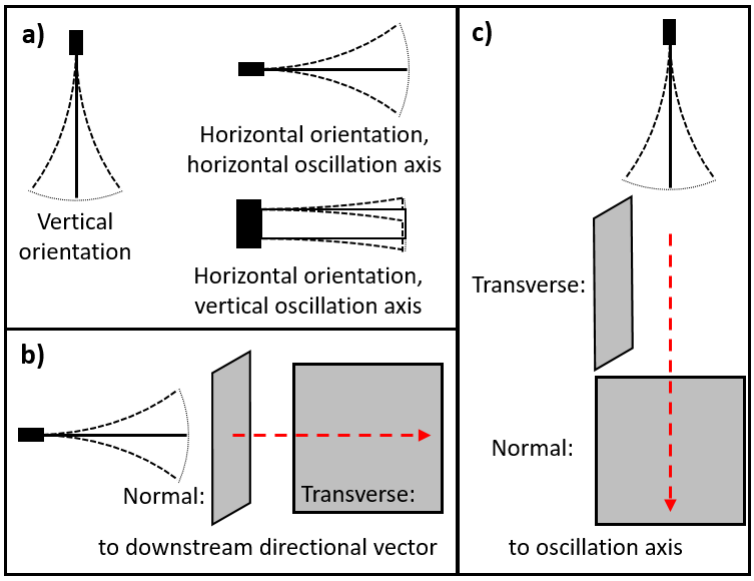

Figure 8: PE fan orientations

4. For a horizontally orientated PE fan and a vertically orientated heat source, is the heated surface normal or transverse to the DDV (Figure 8b)?
5. For a vertically orientated PE fan and a vertically orientated heat source, is the heated surface in the plane normal to the axis of oscillation (Figure 8c)?

Lin [23] compared two setups, a horizontally orientated PE fan oscillating around the vertical axis and a vertically orientated PE fan, both with the heated surface normal to the DDV and discrepancy between the results was small. Downstream airflow was found to be large compared to the natural convection driven by buoyancy and experimental heat transfer enhancement values deviated a maximum of 16%. It is reasonable to conclude that, whilst gravitational effects are not negligible in design optimisation process, they should be considered secondarily to other factors, such as proximity to a heat source.

Liu *et al.* [31] carried tests with horizontally orientated PE fans and heated surfaces, as shown in Figure 9. Oscillation axis, amplitude and blade tip position

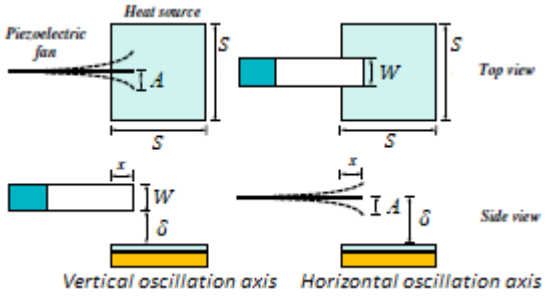

Figure 9: PE fan and heated surface orientation for experimental studies presented by Liu *et al.* [31]

were varied to produce Figure 10, which considers the subsequent heat transfer enhancement. The peak enhancement ratios suggest the superior oscillation axis is dependent on the amplitude, and is optimised at different positions. Additionally, greater decay occurs away from the optimised state when a vertical axis of oscillation is implemented. Both observations can be attributed to airflow entrapment. In the vertical axis of oscillation case, this is between the fan blade's lower edge and the heated surface, which becomes increasingly apparent as x/S is increased.

3.5. Displacement from a Heated Surface

Figure 5 [23] shows heat transfer enhancement to have proportionality with separation distance from a surface normal to the DDV. The same trend is reported by Sufian *et al.* [33] [34] [35] with the separation distance ranging from 1.2mm to 20mm. A 30%, 60% and 90% reduction in separation distance increases heat transfer by 8.4%, 18.6% and 31.3% respectively. This relationship is well established, and can be explained by considering the fundamental airflow. Lei *et al.* [30] demonstrate that separation distance increase has an adverse effect on vortex strength and flow field turbulence at the heated surface for such a setup. Mass and heat transfer would be reduced as a result, explaining from the near vicinity. Quantification of vortex strength would be valuable for further developments in this field.

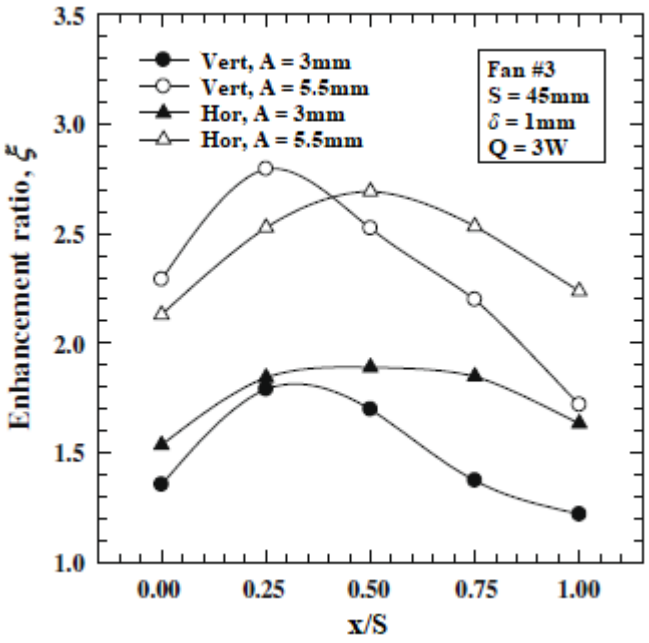

Figure 10: Heat transfer enhancement from a heated surface as orientation, amplitude and surface coverage are varied [31]

Counter to this, Kimber *et al.* [36] showed that at a very small separation distance, 0.085mm, the peak heat transfer coefficient is considerably smaller than when it is increased to 2.1mm and 4.25mm. It appears the relationship is more complex, and an optimal separation distance exists where the best compromise between vicinity. The entrapment of air when the blade is in a state of moderate or high confinement is a theme in a number of topic areas, and must be considered here. It is clear that benefits of increased turbulence at the surface become outweighed by the adverse effects of entrapment, namely reduced airflow away from the surface, when separation distance is reduced past a certain point. Logic suggests blade width and amplitude would be the key parameters defining this point, but further investigation is also required here.

The evident importance of blade width on optimal separation distance has been introduced, and can be visually observed in Figure 11, which shows steady state heat contour maps of a heated surface cooled by three PE fan blades

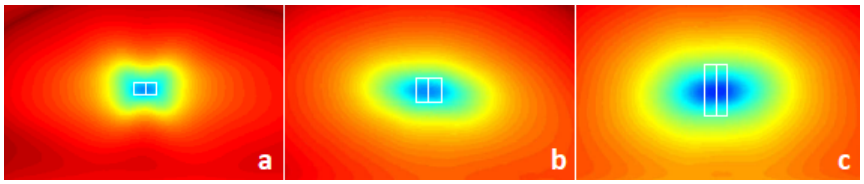

Figure 11: Steady state heat contour maps of a heated surface: a) W=6.35mm, δ/A=0.75, b) W=12.7mm, δ/A=2.75, c) W=25.4mm, δ/A=4.75 [27]

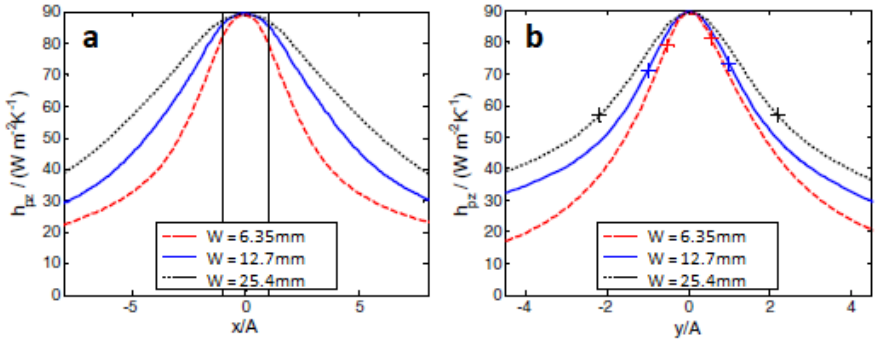

Figure 12: Heat transfer from a heated surface caused by PE fans with three different blade widths, at specific separation distances, along (a) the horizontal and (b) the vertical centrelines [27]

of varying width [27]. A unique approach led Kimber and Garimella to find the dimensionless separation distance, δ/A, at which quantitatively similar heat contour maps were produced. Heat transfer coefficients taken along the vertical and horizontal centrelines from each are plotted in Figure 12, where it can be seen the maximum heat transfer coefficients are identical.

Heat transfer is determined to be a function of the contour shape, within the region of oscillation [27]. Expressing performance by contour shape eliminates blade width as a variable from analysis. [27] proposes 2D modelling through the blade mid-plane would be satisfactory for analysis on the oscillation envelope. [24] states the importance of blade edge effects on the air movement in the wider domain, and width must be considered away from the oscillation envelope, as shown by the varying rates of decay in Figure 12. 3D modelling is therefore necessary for work also documenting the far field.

The relationship between separation distance and induced heat transfer is very different considering a heated surface transversal to the DDV. For a setup similar to the horizontal, x/s=0 case shown in Figure 9, a separation distance increase from 6.11mm to 10.8mm is found to allow greater airflow across the heated surface and increase heat transfer by 4% [37]. Again, therefore, confinement is the factor limiting achievable heat transfer. It will be discussed more thoroughly in Section 3.6.

3.6. Piezoelectric Fan Confinement

Sufian *et al.* [35] considered a heated surface normal to the DDV, whilst confining the blade to varying degrees with side walls. Optimal performance was found when distance from the heated surface was minimised. At large separation distance (5mm), the system performs best with no confinement. For a smaller separation distance (1mm and below) however, an optimal level of confinement is shown to exist.

Ma *et al.* [49] used a PE fan to induce flow through a heat sink, as shown in Figure 13. Temperature drops on the side walls and base are displayed in Figure 14. Reducing the height, δ, of the blade from the heat sink base improved performance. Parallels can be drawn between these results and those displayed in Figure 10, suggesting that whilst confinement may have an effect, the underlying relationships regarding heat transfer optimisation are still valid. Considering results from the vertical oscillation axis as equivalent to heat transfer from the heat sink base, both cases are optimised at low x/L ratios, 0.25 and 0.3 respectively. Using the same parallels to compare the horizontal oscillation axis and heat transfer from the heat sink side walls, both heat transfer from both setups is maximised at x/L=0.5. Similarity is also evident comparing the two studies' dataset shapes.

Looking now at the airflow, rather than heat transfer enhancement, it is possible to infer further relationships by studying the result of varying the parameters shown in Figure 15 [29] [38]. Consideration is once again given to the primary desirable feature of PE fans, their low power requirements.

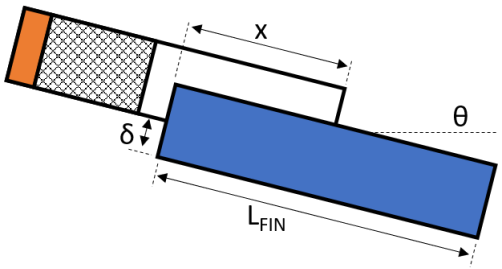

Figure 13: The geometric setup used by Ma *et al.* [49]

For ε <0, the sidewalls have no effect on generated airflow when a g >2mm, whilst substantial enhancement is observed when g <2mm. Additional power is required to maintain the blade's amplitude whilst g <5mm, with demand exponentially increasing as g is reduced. The additional power requirement can be attributed to the added mass from the surrounding fluid, this is verified by observing the decreasing resonant frequency as g is reduced, and this cost always outweighs the benefits of increased thrust from an efficiency standpoint [29]. At small g, peak thrust is generated when ε=0mm, and reduces uniformly as ε is increased, either positively or negatively. For ε ≥0mm, the power requirement when g=1mm and g=2mm is identical. Therefore, a situation exists where thrust can be enhanced at no additional power cost. This phenomenon has not been fully investigated, but could provide additional methods of optimisation for many practical PE fan assembly designs.

Kimber *et al.* [16] trialled a PE fan in an enclosure. Enclosure depth and PE fan geometric properties were maintained, whilst height and width were reduced from 80×40mm to 50×25mm and 30×15mm. Power requirement to maintain oscillation amplitude was increased by 2%, 10% and 40% respectively, compared to unconfined oscillation. The pressure within the enclosure is shown to increase as the fan is confined, and the enhanced damping caused by this explains the increased power demand. Airflow generation was relatively unaffected by the confinement, suggesting that attainable flow rate is a function of only PE fan characteristics, independent of side wall proximity.

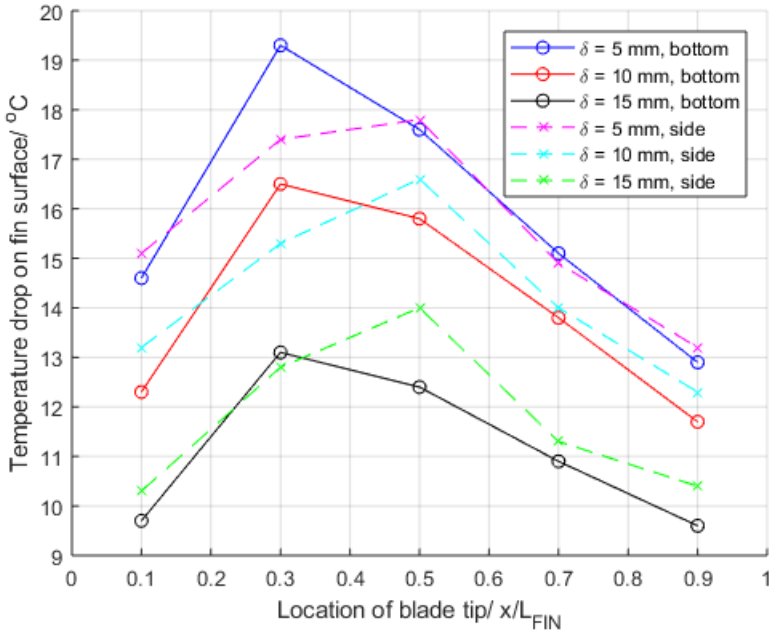

Figure 14: Surface temperature drop at different PE fan heights and positions within a heat sink [49]

Stafford and Jeffers [39] found results contradicting conclusions drawn in [16], by confining a blade above and below its faces, down to the oscillation envelope. Generated airflow is reported to be 20% of that achievable with an unconfined blade. Air entrapment has been considered across the research in this area, but the conflicting conclusions suggest work focusing specifically on airflow generation in confined circumstances would be beneficial to the subject.

3.7. Piezoelectric Fan Oscillation Transversal to Channel Airflow

Figure 16a shows a PE fan, oscillating transversally to channel airflow, used by Florio and Harnoy [50], to enhance turbulence around a heat source. This introduces a largely unexplored topic area, using PE fans to induce turbulence at a specific point. Theoretically, the heat transfer from a surface in a channel flow will increase in proportion with the flow rate. However, with such a setup, this enhancement factor could be dramatically improved as mass transfer at

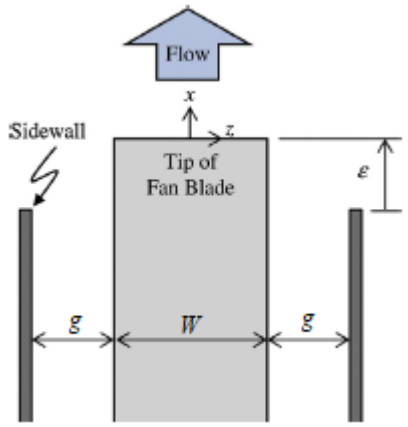

Figure 15: Key parameters studied by Eastman and Kimber [38]

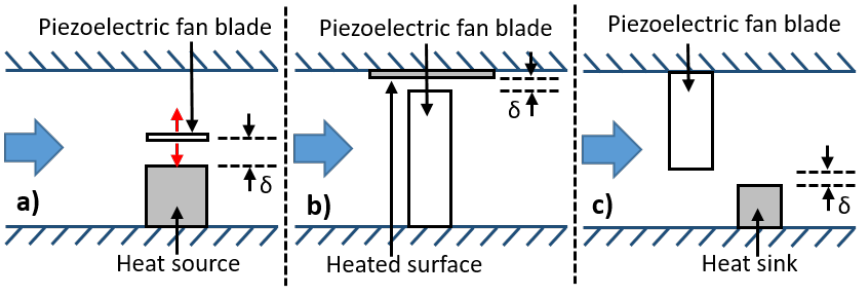

Figure 16: PE fan and heat source orientations, with oscillation transversal to channel airflow

the ideal point is increased. Results are to be expected, showing heat transfer from the top surface improved with reduced separation distance, and also with increased oscillation frequency and amplitude. Li *et al.* [19], considered the setup shown in Figure 16b. The smallest separation distance under test yielded the best heat transfer from the surface.

Returning to the system in Figure 16a, further optimisation can be achieved by moving the PE fan blade upstream by a distance of 1.5 blade widths, since heat transfer from the left and right heat source walls was also considered [50]. The generated turbulence induced substantial mass and heat transfer on the left hand surface and heat transfer from the entire system was improved by 52%.

Jeng and Liu [51] found, considering the setup shown in Figure 16c, that a square pinned heat sink facilitates greater heat transfer, compared to a conventional finned heat sink. Heat transfer enhancement is most substantial when the Reynold's number of the channel airflow is smallest, because of the relative increase in turbulence. This is an essential consideration, which limits the application range of such designs. A study of data in the published literature suggests that the blade tip maximum speed must be an order of magnitude greater than the average channel flow air speed for significant benefits to be observed (greater than 10% enhancement). Above air velocities of $1 m.s^{-1}$, therefore, the PE fan technology required does not yet exist.

4. Piezoelectric Fan Arrays

Single PE fans are unable to generate sufficient airflow to replace conventional air movers, such as axial fans, which are used in a wide range of power electronics. To provide a viable alternative, PE fan arrays must be used. Orientation, face-to-face (FTF) or edge-to-edge (ETE), and oscillation phase are two key design variables. Additionally pitch, as a function of amplitude, governs a wide range of the generated flow field characteristics.

4.1. Edge-to-Edge Orientation

Vortex formation from ETE, in-phase oscillation is similar to that of a single blade [52]. In use in an unconfined space, therefore, the design does not appear logical. Manufacturing time and part count could be reduced by using a single, wider PE fan blade. Strength is added to this argument by results in Figure 17b [53], which shows oscillation amplitude at a given power input is reduced during in-phase oscillation.

In counter-phase, results are more promising. Oscillation amplitude is enhanced by air-coupling and, assuming proportionality with induced airflow [26], logic suggests a PE fan array's performance would increase by a factor greater than N, the number of blades in the array. This hypothesis is not backed up

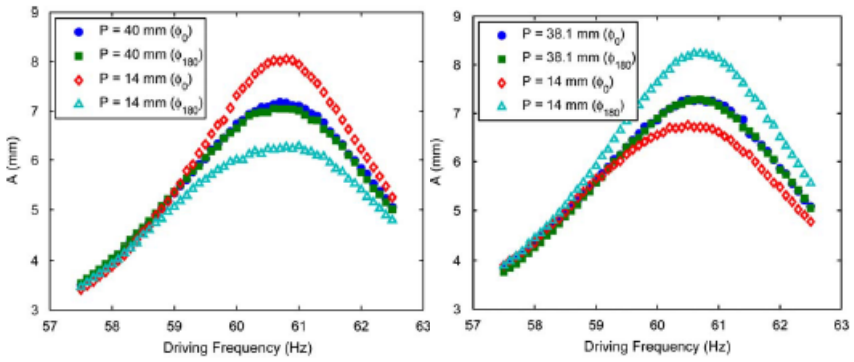

(a) FTF oscillation

(b) ETE oscillation

Figure 17: Oscillation frequency vs. amplitude for two PE fans oscillating in phase and counter-phase at a large and small pitch [53]

by results published by Huang and Fan [52]. Results show, when $^{P}/_{W}$=1.79, in-phase oscillation creates the greatest air velocity magnitudes at a surface normal to the DDV, whilst counter-phase is actually less effective than 30° or 90° out-of-phase oscillation. Pitch variation is likely to explain discrepancy between these two sets of results, as the counter-phase model is unlikely to optimised at the same pitch as the in-phase approach.

The issue with ETE orientation is the eventual geometry of the array: the width greater than the sum of each blade width, W, and the height equal to just the oscillation envelope. This, for many applications may prove impractical. FTF orientation may prove to be a favourable alternative in this respect, and for this reason has been investigated more thoroughly.

4.2. Face-to-Face Orientation

In-phase, a single vortex, rotating as the vortex behind the trailing blade, is formed between the two blades through each half cycle of in-phase oscillation [34]. Interaction between the blades is at a minimum when in-phase, progressively increases to a maximum level when in counter-phase [54].

Sufian *et al.* [34] found, through numerical modelling of two face-to-face (FTF) blades oscillating in counter-phase, that vortices induced on the outside

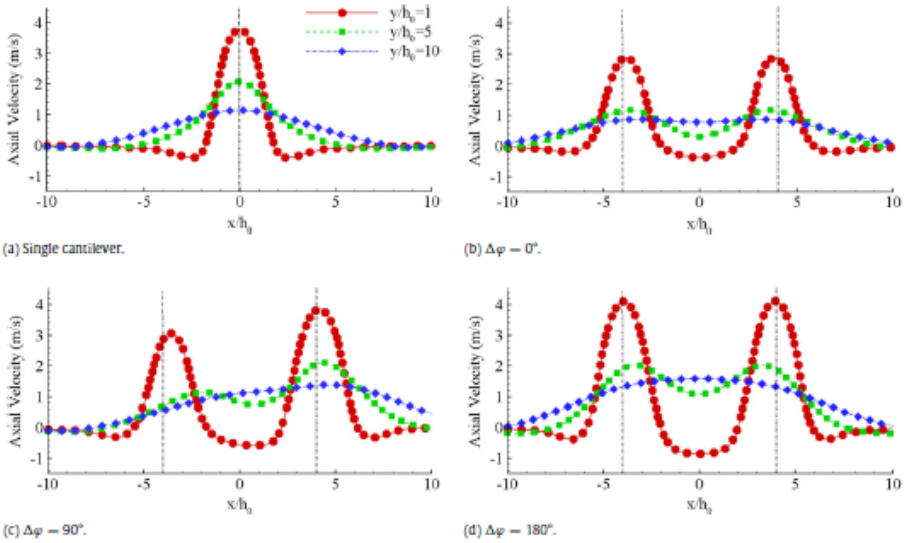

Figure 18: Downstream velocity profiles generated by: (a) a single PE fan), a pair of FTF PE fans at a pitch P=8A: b) during in-phase oscillation, c) 90°out-of-phase oscillation and d) counter-phase oscillation [54]

faces of the two blades are similar to those observed with a single blade. The flow field between the blades is complex. Each blade, during the opening period, generates a vortex behind it, counter rotating to one another. Choi *et al.* [55] report these vortices, fully grown, to be $3A$ - $4A$ in diameter.

A large adverse flow is formed during the closing period of the cycle [34]. Choi *et al.* [54] show similar findings in Figure 18d, where a negative axial velocity can be observed between the two blades. Ihara and Watanabe [21] also report such results when pitch (P) is greater than the peak-to-peak amplitude ($2A$), but find that no adverse flow is induced when $P = 2A$.

An extensive study of the effect of pitch variance has not being carried out across all reasonable ranges of pitch, and it is therefore difficult to highlight the pitches at which maximum or minimum downstream velocities or flow rates occur. At low pitch, $P < 4A$, data suggests optimal downstream flow rate is achieved when pitch is minimised, $P = 2A$. It seems reasonable to assume this is related to the absense of adverse flow at $P = 2A$. In all cases the peak

downstream flow velocity is less than that produced by a single PE fan blade [21].

At larger pitch, $4A \leq P \leq 8A$, a very differnt relationship is reported. Figure 18d [54] shows counter-phase oscillation at $P{=}8A$ generates superior peak downstream velocity to a single PE fan, shwon in Figure 18a. Performance improves from the minimum tested pitch, $P{=}4A$, and is said to be maximised in the region $6A \leq P \leq 8A$ [55], where two fully formed vortices are able to occupy the space between the blades.

Coupling describes the degree to which the two blades are affected by one another's motion in the air, and in the counter-phase, FTF case, it is always detrimental to the blades' amplitude. Figure 17a [53] shows the uncoupled state for counter-phase FTF oscillation lies at $P \leq 5.7A$. Below this, the oscillation amplitude is reduced, as the blades struggle to either compress (in the closing period) or expand (in the opening period) the air between them. It is logical to infer that the degree of coupling, and therefore amplitude reduction, is increased as pitch is decreased. Compiling the evidence in the literature, a region is found, $5.7A \leq P \leq 8A$, where counter-phase oscillating blades appear decoupled, but their vortices are able to increase downstream airflow. The quantitative pitch values of this region have not been determined, and they are likely to be a function of other variables in addition to amplitude. Work focusing on this region would be of great benefit to future development to the thermal management technology.

At low pitch, counter-phase oscillation may still have an application. High levels of turbulence are observed by Schmidt [56] when $^{P}/_{A} < 4$, where vortices cannot become fully formed and instead mix. This turbulence may be used to enhance heat transfer from a heat source in the very near vicinity of the blade tips, and may provide the basis for an evolution on the design for hot spot cooling, which has in the past been undertaken by a single PE fan blade.

Based on the available evidence, counter-phase blades should be positioned at a pitch of $6A \leq P \leq 8A$ to optimise downstream velocity performance. This is not the case for in-phase blades where, in the same pitch region, a detrimental

coupling effect occurs. This can be seen by comparing the peak velocities in Figure 18b, shown for the case of P=8A, with the peak velocity produced from the single PE fan (Figure 18a). In-phase oscillation is optimised at low pitch, $P \leq 4A$, where the generated downstream flow rate is more than double that induced by a single PE fan [21].

Coupling is once again the architect of this phenomenon, this time beneficially. The momentum gained by the air moving between the two blades enhances amplitude at any driving frequency. Kimber *et al.* [53] demonstrated for such a setup that air coupling is capable of increasing the amplitude of each blade by 16%, when compared to the oscillation of a single PE fan blade. Another study, this time comparing in-phase and counter-phase oscillation at the outer reaches, P=5A, of the coupling region, found the in-phase oscillation amplitude to be 25% greater [34].

Quantitative understanding is essential to harness the full capacity of coupling, and once again the pitch is the essential parameter: coupling is increased as pitch is reduced. Figure 19 [53] shows that at a pitch of 40mm (P/A=5.7), representing the uncoupled state, oscillation amplitude is 33% and 23% lower than at pitches of 8.4mm (P/A=0.92) and 5.0mm (P/A=0.48) respectively. The resonant frequency increases as coupling strengthens, from 60.2Hz at a 40mm pitch to 60.6Hz and 60.9Hz at 8.4mm and 5.0mm pitches respectively.

Beneficial coupling can be used to reduce power demand [17]. Qualitatively, for a given oscillation amplitude, an array of N PE fans operating at optimal pitch will require less than N times as much power as a single PE fan. To develop upon this, it should be considered that beneficial coupling may be used to simply improve downstream flow rate. The single biggest problem facing PE fans in industry, at present, is their inability to move large volumes of air effectively, and as such they are not currently implemented on a wide scale. The improved performance by an array of PE fan blades, each operating at it's maximum power input, may open up more application areas where they can replace conventional air movers.

The discussed results conclude that at small pitch, in-phase oscillation should

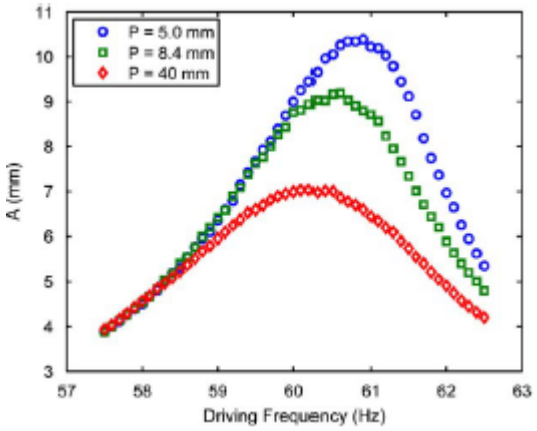

Figure 19: Oscillation frequency vs. amplitude for two FTF, in-phase PE fans, at a range of pitches [53]

be used, but that a threshold pitch is reached where counter-phase oscillation becomes preferable. Discrepancy is found by instead analysing the heat transfer from heat sources positioned in the generated flow. At P=6.25A, above the threshold pitch, counter-phase oscillation is found to be 14-18% less effective than in-phase oscillation, across a range of separation distances, δ, from the blade tips to the heated surface [34]. Considering the relationships between downstream flow rate and heat transfer enhancement, which are widely established in the research field, these findings provide a staggering contradiction. The heat surface in the presented model is relatively close, $^{\delta}/_{A}$ <<1, and therefore perhaps an air entrapment issue with counter-phase oscillation. In addition to threshold pitch, evidence suggests their is a threshold separation distance, below which in-phase is preferable.

At small pitch, where in-phase is preferred, optimisation through heat transfer assessment is as expected considering established relationships translated from single PE fan results. An optimum separation distance exists which is demonstrated in Figure 20 [17], considering $^{P}/_{A}$=1.25, close to the optimised state, $^{P}/_{A}$=1.5. Peak performance occurs at δ=1mm. Furthermore, a large separation distance allows for better heat transfer from far regions of the sur-

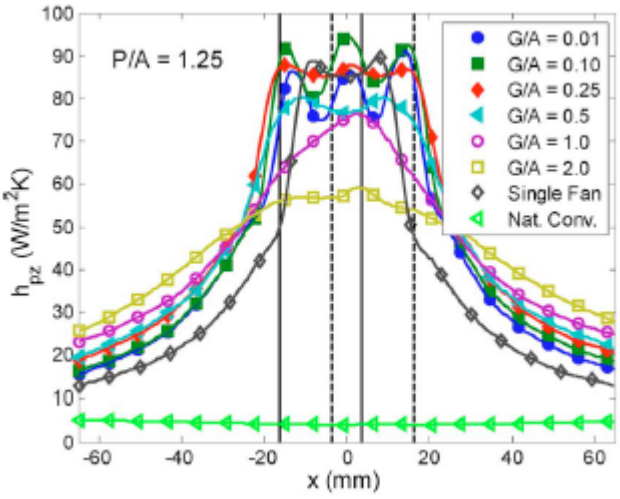

Figure 20: Local heat transfer, induced by oscillation of two FTF in-phase PE fans, across the horizontal centreline of a heated surface at six separation distances [17]

face. 15mm outside the oscillation envelope, the δ=20mm configuration returns optimal performance. These relationships hold true at other $^{P}/_{A}$ ratios.

4.3. Orientation Comparison

In-phase, FTF oscillation is found to enhance heat transfer by 6% compared to ETE [33]. This is down to the increased surface area cooled by this setup, as shown in Figure 21 [33]. Kimber *et al.* [40] verify these conclusions with the same setup and a separation distance of 1.59mm. A 2% and 21% enhancement is found, compared to ETE orientation and a single PE fan respectively. As previously highlighted, these results, coupled with the design impracticalities of ETE orientation, suggest FTF to be perferable in all but a few specific cases.

A third design possibility, a PE fan array 'stack', combining both orientations and their respective favourable characteristics, has not been considered to date, but may well evolve the optimisation process of PE fan arrays in the future. Whilst the single PE fan research field is very well understood, array's are still some way off full optimisation, and the topic lends itself to more complete design innovation. Examples of this methodology are introduced in the following

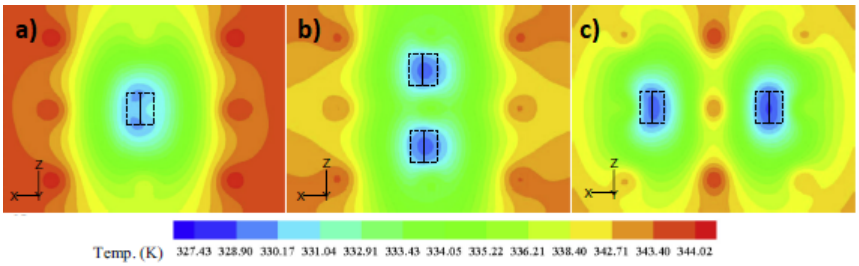

Figure 21: Thermal profile of a heated surface, under cooling from a) a single PE fan, b) two ETE, in-phase PE fans and c) two FTF, in-phase PE fans [33]

section.

4.4. Novel and Innovative Design

Ma *et al.* [57] [58] presented a five blade array orientated FTF and coupled by magnets attached close to their blade tips. The entire array is driven by a single PZT strip, attached to the middle blade. The blades oscillate in-phase, each to an amplitude almost equivalent to that achieved by a lone PE fan. Taking total amplitude as a measure, the array outperforms a single PE fan by 275% for a given power input.

System apparent stiffness, K_{mag}, is derived considering the magnetic coupling and has a direct relationship with resonant frequency. Assuming all other system properties are constant and represented by a coefficient, B, apparent stiffness governed by Equation 6 [58]. A 15% to 25% reduction in resonant frequency is observed as pitch is increased from 11mm ($^{P}/_{A}$=1.4) to 29mm ($^{P}/_{A}$=3.6).

$$K_{mag} = \frac{B}{P^3} \tag{6}$$

Use within a heat sink is a very relevant topic area as, to reiterate a point, it opens up a range of new applications for PE fans. Arrays are most commonly orientated ETE when operating within a heat sink [41]. The blades in such a setup are not coupled through air and can be treated as single blades for optimisation. From analysis in Section 3.6, it can be inferred that FTF orientation

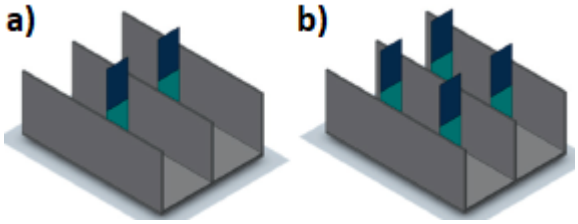

Figure 22: A two (a) and four (b) PE fan array designed to operate within a heat sink [59]

does not make best use of the surrounding heated surfaces.

Shyu and Syu [48] developed a single blade, geometrically designed with four 'fingers' which then fit between the five fins of a heat sink in. The assembly performed optimally when positioned centrally and with minimal seperation from the heat sink base. Optimisation is limited to an extent: characteristics of the individual fingers cannot be altered independently due to the detrimental effects to the operational characteristics as a whole. Tseng *et al.* [46] considered a similar blade, this time with a nine fingers. The part count and manufacture complexity is reduced, and such a solution is ideal for certain applications.

Sufian and Abdullah [59] trialled the setups shown in Figure 22, with the PE fans operating in-phase with one another. The four blade array (b) enhances heat transfer by 180% and 35%, compared to natural convection and the two blade array (a) respectively. The four blade setup performs best at $^{P}/_{A}$=7. Considering the optimal FTF $^{P}/_{A}$ ratios reported, side wall presence appears to have a measurable effect on the best pitch. Side wall proximity was not varied through the study and an investigation into this variable would more in depth analysis in the field.

Petroski *et al.* [60] presented a complex heat sink, incorporating and encasing two decoupled PE fans. The base of the heat sink is thick to allow good conductive heat transfer from the heated surface upon which it is seated. The focus is enhancement of heat transfer from a surface rather than the hot spot cooling typically associated with single PE fan operation. Performance, compared to natural convection driving heat transfer from a finned heat sink, can be improved by 400%.

5. Numerical Modelling of Piezoelectric Fans

Computational fluid dynamics (CFD) is becoming ever more relevant in research around the topic of power electronic cooling [61], and recent PE fan research has followed this trend. The most relevant theoretical studies are able to apply findings to a specific application and experimental validation of numerical model is essential for credible conclusions to be drawn.

Numerical modelling of PE fans has been common since the turn of the century, with the required hardware and software becoming increasingly available. A domain would include a single or array of oscillating PE fan blades in a certain orientation. A heat source is often included, and other geometric restrictions may also be considered. Studies focusing on the generation of air flow by an oscillating blade prefer a large domain containing no restrictions or heat sources. The transient model is setup to resolve by applying a form of the Navier-Stokes equations, justifiable assumptions and boundary conditions.

For engineering applications, traditional CFD was primarily developed for steady, high-speed flows in the framework of Reynolds-averaged Navier-Stokes (RANS) modelling approach. Numerical simulations of fluid flow and heat transfer induced by PE fans are challenging because the flow is intrinsically unsteady due to the fan oscillations and low-speed entailing turbulent flow. High-fidelity numerical approaches such as large-eddy simulation (LES) and direct numerical simulation (DNS) [62] may provide powerful tools to investigate this type of flow, but they are not widely used at present due to the associated computational costs. In existing studies, less demanding commercial packages based on RANS methods are most often used.

5.1. Model Setup

Several steps of consideration must be taken to setup a model fit for a specific application. These are discussed below, based on summarisation of the relevant papers reviewed.

The majority of reported models are resolved through the finite volume method (FVM), although there are examples, such as work reported by Florio

and Harnoy [50], of finite element method (FEM) solvers in use. Conservation of the Navier-Stokes equations across each control volume is inherent to the FVM but not necessarily for the FEM, and it therefore is less stable in certain scenarios [63].

Several assumptions are made to simplify the Navier-Stokes equations, which govern the fluid dynamics in the models. Incompressible flow is assumed in all relevant studies, since the pressure gradients are not substantial. In some 2D cases [15] [37] [64], buoyancy is also neglected, since gravity is normal to the model's plane. Radiative contributions of the heat source are also neglected (where relevant). Two studies [35] [41] have shown this assumption to be a contributor to the eventual error between the model and validation experiment, as discussed in Section 5.3.

The majority of recent studies have been carried out assuming turbulence in the fluid domain. Reynolds number in the blade tip vicinity is not documented by authors, although the presence of turbulence is widely accepted. In the numerical model, a scheme to define turbulence close to the blade tip is essential. Four schemes are documented in the literature: the shear stress transport (SST) k-ω model [19] [35] [41] [44], the standard k-ε model [20], the renormalisation group (RNG) k-ε model [30] and the large eddy system (LES) model [24].

The SST k-ω model is often preferred and appropriate for both near and far-field zones [65] [66]. The standard k-ε model is used when the flow is assumed to be very turbulent [67]. This is valid, since Choi *et al.* [20] concentrate on blade tip vortex. The RNG k-ε model is a development of the standard k-ε model. It includes the effect of swirl on turbulence, which must be considered for vortex generation, and an additional term to improve rapidly strained flow accuracy [68]: relevant given the close proximity of the heated surface considered by Lei *et al.* [30].

Bidakhvidi *et al.* [24] used the LES model, and state that the intense mixing observed when the vortices interact is not produced by other turbulence models. It is interesting to observe the LES model is not more widely used in existing literature considering this analysis. The requirement for additional computa-

tional capacity is likely to limit the model's usage [63], but with computational advancement at a high rate the modelling method is likely to become more popular in the near future.

Computational limitations has also led some work to be produced assuming laminar flow [15] [37] [64]. Florio and Harnoy [50] highlight it as a source of error and conclude that their solution will represent a low-end estimate for the PE fan's cooling capacity. With continuing technological advancements, the laminar assumption will become increasingly obsolete in the research field.

The chosen time step of a model is based on a compromise between computational demand and accuracy. Approximately 100 timesteps per blade oscillation (TPO) cycle is most common, although enhanced resolution has been preferred on occasions. Bidakhvidi *et al.* [24] chose 471 TPO, and referenced the magnitude of mesh movement to justify the decision: large movement in a single iteration can lead to poor quality meshes and even negative volumes. 833 TPO were implemented by Florio and Harnoy [50], since their oscillation frequency range was very low, ranging from 4Hz to 24Hz. By contrast, Acikalin and Garimella [15] reported a trial of both 40 and 100 TPO in their model, and found that the resolved solutions' system temperatures varied by 0.050°C. As few as 2,000 [30] and as many as 10,000 [33] [44] [59] time steps are reported in the reviewed literature, representing 19.5 and 100 complete oscillations respectively. Concluding from literature, 20 complete blade oscillations is the minimum reach a repeating transient steady state.

2D models reduce the required computation to resolve a numerical model but rely on assumptions that could devalue the quality of the solution. 3D domains allow more thoroughly solution analysis, but require additional computational capacity and typically take longer to resolve.

The 2D domain is most often positioned in the blade mid-plane, where weighted blade edge effects eliminate one another and be diregarded [24] [30] [37] [64]. Florio and Harnoy [50] describe a circumstance where natural convection is moving air across the face of the blade. A plane end-on to the blade tip is necessary in this case to describe the model in just 2D.

Examples can be found where 2D models that have been experimentally validated, as discussed in Section 5.3. Abdullah *et al.* [37] report 11% discrepancy between experimental and numerical surface heat transfer coefficients. The model setup is relatively simple, with only 15,575 elements, an assumption of laminar flow and first order accurate upwind discretisation. Rigorous reverification of the model would be appropriate if the geometric or thermal characteristics are adjusted, given these simplifications.

Acikalin *et al.* [69] conclude that 3D effects in real enclosures are not negligible. This remark is backed up by Bidakhvidi *et al.* [24], who analyse PE fans in 2D and 3D domains. This was done by deploying the 2D plane from which the numerical model was resolved at different points across the PE blade's width, and deriving the 2D velocity vectors from the 3D model to produce comparable data. In this case, turbulence was described by the LES model, discretisation was second order accurate, and 1,500,000 (2D) or 15,000,000 (3D) elements made up the mesh. Additionally, the iteration count per blade oscillation was very high, at 471.

Bidakhvidi *et al.* [24] used highly refined 2D and 3D models to demonstrate the importance of blade edge effects which cannot be replicated in the 2D domain. The 2D solution is chaotic, dominated by the many vortices failing to break out during one sweep of a blade's oscillation. By contrast, the 3D model is dominated by the familiar large vortex formation behind the blade's trailing edge. Correlation between the 2D and 3D models is achieved by increasing blade width beyond relevant dimensions, to negate the edge effects.

Evidence suggests a better model can be created in a 3D domain and studies using such models have become more common since 2014, as hardware and software enhancements have increased viability. Advancements to the way in which numerical solutions can verified will further benefit 3D models over their 2D counterparts.

5.2. Boundary Conditions and Mesh Characteristics

Blade motion is most often defined through theoretical theory, using Equations 1 and 3 [18] [19]. This neglects the impact of the PE actuators on the blade's motion and the physical effects of the clamp limiting the air flow in the fluid domain. Bidakhvidi *et al.* [24] conclude these assumptions are valid since the region of interest, where vortex formation occurs, is the free end. The blade's displacement close to the clamped end is very small compared to that at the free end, and therefore the effect of the actuator on the blade's oscillation is negligible [15]. The driving coefficient, D_c, describes the blade's amplitude and can be set to replicate any specific PE fan in the model. Strong correlation between experimental findings and the numerical governing equations is reported by Choi *et al.*.

Equations 1 and 3 can be used to describe the motion of any PE fan as they define the motion through operational characteristics, assuming the coefficient β is known. Empirically derived equations can be used in place of Equation 1. They are preferred by authors when only a specific PE fan blade motion is required for numerical modelling as they do not assume negligible resistance and PE actuator effects on the motion, but are limited to describing just one set of PE fan geometric and material properties.

Li *et al.* [19] present Equation 7, an empirically derived function describing their PE fan's blade shape at the point of maximum displacement, where x is the distance along the blade from the clamped end, $Y_{Jun2017}$ is the displacement of the blade from the oscillation midpoint, which can be then used in Equation 3 to describe the blades motion with time. The coefficients p_1 through to p_5 are defined for multiple voltage inputs in the report [19]. A different function, Equation 8, is reported by Acikalin and Garimella [15] to describe a different PE fan blade's mode shape at the point of maximum displacement. Implemented into the model's domain, the blade is best defined as an adiabatic, thin wall allowing no heat transfer [30] [35] [37] [41] [64].

$$Y_{Jun2017}(x) = p_1x^4 + p_2x^3 + p_3x^2 + p_4x + p_5 \tag{7}$$

$$Y_{Acikalin2009}(x) = -42.3402x^2 + 33587.5x^3 - 2.7317 \cdot 10^6 \cdot x^4 \\ +9.05342 \cdot 10^7 \cdot x^5 - 1.2653 \cdot 10^9 \cdot x^6 + 6.34496 \cdot 10^9 \cdot x^7 \quad (8)$$

Mesh resolution is driven by a compromise between result accuracy and model run time. The variance in element array size is large across the literature. 10,000 to 20,000 elements are common for 2D models resolved in a few hours [15] [37] [64], whilst finer meshes with up to 90,000 elements are also reported [20] [30]. With a 3D domain, at least 450,000 elements have been used across the literature, with up to 15,000,000 [24]. A 2D domain may have finer node spacing, but contain far fewer elements than an equivelent 3D domain. Acikalin and Garimella [15] considered both 2D and 3D domains. 14,500 nodes generated the mesh in the 2D domain, which was then extruded 32 times in the third dimension to create an array of 450,000 nodes. The model took six weeks to resolve.

In 2D, triangular elements are often preferred [20] [30] [37] [64], although Florio and Harnoy [50] report a quadrilateral element mesh. In 3D, mesh generation is more complex and several different polyhedrons can be found in the same domain. 'Hybrid grids', a combination of tetrahedral and hexahedral volumes are used by Sufian and Abdullah [59]. The oscillating blade is defined as a surface in a 3D model and, along with domain boundaries, is most often meshed with quadrilateral elements [59].

The moving boundary replicating the blade demands the use of dynamic meshes, which regenerate with each time step to maintain a suitable mesh as the domain geometry changes. Choi *et al.* [20] designed a mesh with a deforming zone close to the moving blade boundary and a stationary wider domain, and reduced computational demand as a result. A similar approach is documented by other authors, but continuity of outputted values can be adversely affected by the presence of an interface between two different zones in an interior fluid domain.

5.3. Experimental Validation

In general, modelling and simulation can be used to run pre-calculations under experimental conditions, to guide experimental work and to obtain a better understanding of the problem under investigation. In addition, high-fidelity numerical simulations such as LES can obtain results that are of much higher spatial and temporal resolutions than experimental results for a large number of computational cases. More importantly, numerical simulations can also be used to optimise the system design for cooling applications using PE actuators. However, numerical results need to be validated against experimental measurements as there are always assumptions and simplifications in the numerical modelling which can potentially lead to problematic predictions. Comparison to experimental work has allowed authors to validate their numerical solutions using two primary methods which are introduced below.

Quantitative validation is achieved through comparison of numerically derived and experimentally determined heat transfer coefficients from a similar defined system. This method has been used by a large majority of research groups since 2000. Lei *et al.* [30] used such a method for a 2D model. The experimental setup, including a single PE fan providing cooling to a heat plate, was replicated in the numerical model and surface heat transfer coefficients were taken at defined points on the plate. The maximum error was reported to be 15%. The same process has been used to validate 3D models in several publications. Error values are comparable: 15.17% and 17% [59], 11.3% and 15% [35], and 10% and 8% [23].

Huang and Fan [52] demonstrate that a similar method validates their model to a maximum error of 0.68%. The temperature fluctuations across a cooled surface are compared in kelvin and therefore in the region of 300K. Abdullah *et al.* [41] reported an error 1% using the same validation process. The method reduces error resolution, since thermal conditions are not reported outside the 273K to 373K region. Heat transfer from a zone is driven the temperature gradient between itself and the outside conditions, and therefore the ambient temperature should be used as the datum, rather than 0K.

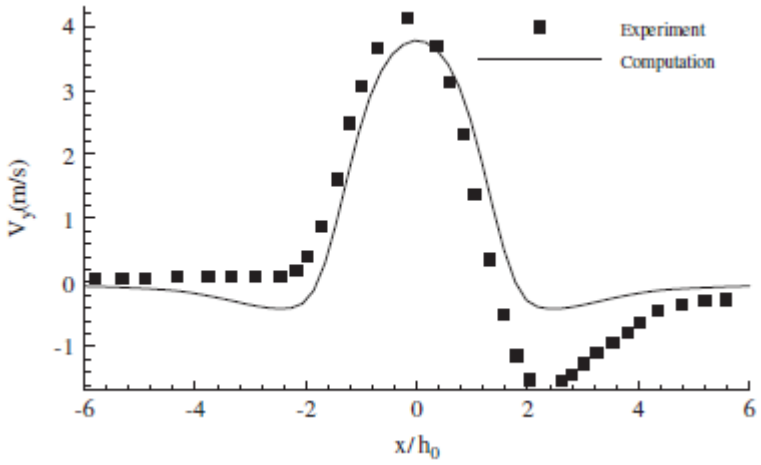

Figure 23: Experimental and computational downstream velocity profiles, averaged over a period of one complete oscillation of the PE fan [20]

Heat transfer or temperature comparison methods output a quantitative error value but limit the degree of validation. Verification requires an equivalent experiment to be carried out when significant parameter variation occurs in the numerical model. A better model can be applied on a global scale: where validation for one geometric and thermal setup would remain applicable as the model's parameters are varied. To achieve this, the phenomena that lead to the heat transfer must be analysed.

Choi *et al.* [20] considered a different approach by analysing the generation of air flow from the blade tip. The time-averaged velocity distribution profiles a set distance downstream are compared, as shown in Figure 23. The two distributions are well matched, although the asymmetric profile produced by the experimental results is not replicated in the numerical solution. Vortex characteristics, specifically size variation and downstream trajectory, were also compared with the numerical data, with strong correlation found. The entire air flow is being analysed through this method, yielding strong qualitative verification. Beneficially, the model can be used to analyse thermally and geometrically dissimilar systems, without the need for further validation.

The method is limited by the required experimental work. Particle image velocimetry (PIV) analysis is necessary to record airflow from a typical PE fan, and is most commonly limited by experimental equipment and computational capacity to 2D. Use of the results for model validation is therefore also confined to 2D.

Each method of validation has considerable limitations. For the former, thorough validation cannot be extended to systems with different geometric or thermal parameters. For the latter, researchers must sacrifice quantifiable error and validation in a 3D domain, despite several studies highlighting the non-negligible 3D effects. Advancements in experimental equipment and techniques, for example as used by Agarwal *et al.* [25], to present PIV results in 3D may provide the basis for global validation in a 3D model.

Lei *et al.* [30] provide the basis for a methodology which may become common in the coming years: validation of computational data through pre-existing experimental results. The research team recreated the experimental setup reported by Acikalin and Garimella [15] in their 2D domain, and comparison of heat transfer coefficients found an error of 15%. The method removes the requirement for expensive and timely experimental work. Florio and Harnoy [50] report a similar process, although quantitative details are not given.

The majority of the reviewed literature reports an error of at least 10%. Abdullah *et al.* summarise the primary error sources, highlighting the omission of radiative effects from their model. This is confirmed by comparing the error value with the experimentally determined radiative contribution. The ambient temperature measurements (experimentally this was done with a single thermocouple, but computationally taken as an average across the relevant region of the domain) and unmatched blade oscillation frequencies are also discussed as contributors.

6. Piezoelectric Fan Applications

PE fan technology has the potential to dramatically reduce the energy demanded by thermal management systems dependent on heat transfer through airflow and convection. Technology that implements liquid cooling or heat dissipation through phase change materials are generally delicate, involving complex designs and therefore expensive [5] [10]. There is a specific need for infrastructures to have low heat generation and effective but low-cost cooling and as a result air-cooled systems are still used in more than 95% of computer technology worldwide. The market for PE fans is therefore very wide [12].

6.1. Competition to Piezoelectric Fan Technology

PE fans are most commonly compared to high-speed axial fans, and evidence suggests PE fans exhibit comparable cooling capabilities for 50% of the power demand [15] [16] [17]. This value is based on the volume of airflow generated by a given power input. Therefore, for certain applications such as hot spot cooling, the technology is highly beneficial. An axial fan solution is most elegant in a situation of confinement, and this is where the implementation of PE fan technology has been less widespread.

High-speed axial fans are able to generate a very large amount of airflow from a comparatively small component. Data suggests a typical axial fan (here the example of taken for a *Delta Electronics Inc.* DC Fan: FFB0412SHN), used for the cooling of power electronics, may generate ten times the airflow of a typical PE fan [70]. The economic cost of ten PE fans renders the technology unviable in its present state for a range of applications in power electronics. Innovation in the PE fan field is therefore ongoing to optimise performance and array design sufficiently, in order to reduce the number of blades required within an electronic assembly [52] [58].

Disregarding the substantial energy demand, axial fans have other operational drawbacks. They generate noise, which is highly disadvantageous in certain markets such as for personal use power electronics. Additionally, their

fundamental design is limited as they require moving parts which inevitably where over time [71].

PE fans do not have any moving components [60]. They operate with negligible noise generation and do not wear with use. The optimisation of geometric and operational characteristics provide an opportunity to further enhance the energy saving of the alternative air-moving technology. Examples have been set out in this review, such as the use of multiple fan blades in an array, and the use of fan blades oscillating transversally to a dominating airflow.

6.2. Energy Consumption

Reducing the energy demand is of paramount importance to sustainable energy utilisation, where there are major challenges in many technological areas. For instance, the growing information and communications technology (ICT) demand is outpacing developments in energy management for the systems. ICT infrastructures are responsible for a significant proportion of electricity consumed, exceeding 1560 TWh and corresponding to 8% of the global demand in 2013 [72].

The world's data centres provide an example of the expanding problem. Their energy consumption has grown at a rate of 11.7% per year since 2000 [6] [7], up to 416.2 TWh in 2016 [8]. However, around 40% of this energy is put towards the cooling systems for the electrical components [13]. This thermal management has most often been implemented with conventional axial fans [9].

Energy consumption has been a secondary consideration for corporations more interested in optimising power density of ICT. This is the case across a wide range of industry sectors, and it is evident that the demand for power electronics has outgrown advances in thermal management systems in the last 30 years [4] [5]. The PE fan is an attractive alternative air-mover for the immediate future [12], providing a possible solution for components generating moderate heat fluxes (1000 - 10,000 $W.m^{-2}$) [12].

6.3. Energy Reduction

It is evident from the quantitative data reported that PE fan technology has the potential to provide enormous energy savings in targeted industrial sectors. This is exaggerated by the wide-scale use of airflow in thermal management systems in the present day and the dominance of axial fans, over which PE fans have clear energy reduction benefits in the highlighted applications.

The specific case of data centre energy usage, along with crude oil consumption, may be analysed to provide an example of the benefits of the implementation of PE fan technology for the cooling of power electronics. It can be approximated using reported data from Khalaj *et al.* that 166.5 TWh is put towards the cooling of data centres worldwide per year [13] [8]. Khalaj *et al.* reference air-moving technology to be a major source of this consumption but do not provide quantitative data. A conservative estimate based on the power requirements of individual servers may be that 30 TWh (around 20% of the energy consumed by cooling systems) is put towards the operation of axial fans per year. Based on data from Garimella *et al.*, this can be reduced to 15 TWh through implementation of PE fan solutions. Approximately 33% of the worlds energy comes from oil [73], and therefore 5 TWh of crude oil energy would be cut each year, equivalent to 2.9 million barrels [73] [74].

Arent *et al.* examine greenhouse gas (GHG) emissions by considering the largest single contributor, carbon dioxide (CO_2), as an example [75]. The same methodology is applied here. 1.25 million metric tons of CO_2 would be released into the atmosphere by burning 2.9 million barrels of crude oil [74]. Just 14.5% of global energy is sourced from nuclear energy and other renewables, the rest coming from alternative fossil fuels [73]. This is therefore a gross underestimate of the potential GHG reduction and environmental benefits that can be achieved by replacing axial fans with PE fans in just one of many industrial applications.

7. Conclusions

Evidence suggests the implementation of PE fan technology will lead to a significant reduction in the power demanded by the thermal management systems of power electronics. Further, the most recent articles and publications have concluded that the critical point has been reached, where rapid innovation in cooling systems must occur to keep up with the advancements in power-density of electronics. PE fans are providing an elegant solution for the immediate future of air-cooling innovation, and further optimisation of PE fans will widen the range of applications in which they are viable. The environmental benefits, in terms of quantity of fossil fuels burnt and GHG emissions, will be substantial should PE fans become a more commonly used air-mover in industry.

There is a wide range of possible parameters that can be varied to optimise a single PE fan for a particular application, concerning the actual PE fan as well as its surroundings. Geometric and material variance is most fundamental, and defines the operational characteristics, frequency and amplitude. The effects of varying these geometric and material characteristics are governed by theoretical equations, and fully understood. The effect of varying a PE fan blade's operational characteristics has been thoroughly investigated and is also well understood. Increasing frequency or amplitude will lead to greater airflow and turbulence at the blade tip. Variance of a PE fan's surroundings is also well understood. For example, heat transfer from a given surface is maximised by minimising the distance between the fan blade tip.

The variance of parameters is less well understood when multiple PE fan blades are considered, and pitch is shown to be central to a face-to-face orientated blade array's operation. In-phase, it determines the degree to which adjacent blades are coupled, and the subsequent increase in oscillation amplitude and airflow generation. Out-of-phase, a number of effects are partially dependent on pitch, including oscillation amplitude, airflow generation, adverse airflow generation and near field turbulence. This topic is of high importance as the single PE fan is not capable of replacing the axial fan regarding many ap-

plications, given the inferior airflow generation from a lone component. Arrays, however, are capable of replacing conventional air movers in moderate heat flux situations, with a significant benefit regarding power consumption.

Numerical modelling is becoming ever more important in the research field, as hardware and software advances at a high rate. The vast majority of work published since 2014 includes at least a portion of numerical modelling. CFD allows optimisation of PE fans for a given application to develop at a far higher rate than purely experimental work, and this is a trend that is expected to exponentially increase in the future.

Numerical methods, at present, are most heavily limited by the quality of validation. Most models rely on validation against just one measurement taken from experimental results, most commonly the heat transfer coefficient from a surface, heat source, or system. Validation through this method is not global: the parameters of a model cannot be varied without the need for, at least the consideration of, further model verification. One example of model validation by comparing the airflow and vortex generation at the blade tip [20] demonstrates that global validation of a model is achievable, although only in 2D. Development of both experimental methods and analysis methods is essential to achieve global validation in 3D, which will be of great benefit to the research field.

Acknowledgements

The authors would like to acknowledge the support of the UK Engineering and Physical Sciences Research Council (EPSRC) under the project grant EP/P030157/1.

References

[1] M. Toda, Theory of air flow generation by a resonant type PVF2 bimorph cantilever vibrator (1978).

[2] H. H. Kolm, E. A. Kolm, Solid state blower (1985).

[3] M. Maaspuro, Piezoelectric oscillating cantilever fan for thermal management of electronics and LEDs - a review, Microelectronics Reliability 63 (2016) 342–353.

[4] S. Mazenq, D. Highgate, S. D. Probert, Electronics cooling using a simple gas-fluidised bed, Applied Energy 34 (2) (1989) 81–88.

[5] S. Mahmoud, A. Tang, C. Toh, R. AL-Dadah, S. L. Soo, Experimental investigation of inserts configurations and PCM type on the thermal performance of PCM based heat sinks, Applied Energy 112 (2013) 1349–1356.

[6] J. G. Koomey, Worldwide electricity used in data centers, Environmental Research Letters 3 (3) (2008) 034008.

[7] J. G. Koomey, Growth in data center electricity use 2005 to 2010, Analytical Press.

[8] N. Patrignani, The Challenge of ICT Long-Term Sustainability, Visions for Sustainability 7 (2017) 54–59.

[9] C. S. Sharma, G. Schlottig, T. Brunschwiler, M. K. Tiwari, B. Michel, D. Poulikakos, Energy efficient hotspot-targeted embedded liquid cooling for electronics: An experimental study, International Journal of Heat and Mass Transfer 88 (2015) 684–694.

[10] Z. Ling, W. Fangxian, F. Xiaoming, X. Gao, Z. Zhang, A hybrid thermal management system for lithium ion batteries combining phase change materials with forced-air cooling, Applied Energy 148 (2015) 403–409.

[11] R. C. Chu, R. E. Simons, M. J. Ellsworth, R. R. Schmidt, V. Cozzolino, Review of cooling technologies for computer products, IEEE Transactions on Device and Materials Reliability 4 (4) (2004) 568–585.

[12] S. V. Garimella, T. Persoons, J. Weibel, L. T. Yeh, Technological drivers in data centers and telecom systems: Multiscale thermal, electrical, and energy management, Applied Energy 107 (2013) 66–80.

[13] A. H. Khalaj, S. K. Halgamuge, A Review on efficient thermal management of air- and liquid-cooled data centers: From chip to the cooling system, Applied Energy 205 (March) (2017) 1165–1188.

[14] L. Newborough, M. Newborough, S. Probert, Electronically commutated direct-current motor for driving tube-axial fans: A cost-effective design, Applied Energy 36 (3) (1990) 167–190.

[15] T. Acikalin, S. V. Garimella, Analysis and Prediction of the Thermal Performance of Piezoelectrically Actuated Fans, Heat Transfer Engineering 30 (6) (2009) 487–498.

[16] M. L. Kimber, K. Suzuki, N. Kitsunai, K. Seki, S. V. Garimella, Pressure and flow rate performance of piezoelectric fans, IEEE Transactions on Components and Packaging Technologies 32 (4) (2009) 766–775.

[17] M. L. Kimber, S. V. Garimella, Cooling performance of arrays of vibrating cantilevers, Journal of Heat Transfer 131 (11) (2009) 1–8.

[18] L. Meirovitch, Analytical Methods in Vibrations, Collier-MacMillan Ltd., London, 1967.

[19] X. Li, J. Zhang, X. Tan, Convective heat transfer on a flat surface induced by a vertically - oriented piezoelectric fan in the presence of cross flow, Heat Mass Transfer.

[20] M. Choi, C. Cierpka, Y. H. Kim, Vortex formation by a vibrating cantilever, Journal of Fluids and Structures 31 (2012) 67–78.

[21] A. Ihara, H. Watanabe, On the flow around flexible plates, oscillating with large amplitude, Journal of Fluids and Structures 8 (1994) 601–619.

[22] N. Jeffers, K. P. Nolan, J. Stafford, B. Donnelly, High fidelity phase locked PIV measurements analysing the flow fields surrounding an oscillating piezoelectric fan, Journal of Physics: Conference Series 525 (2014) 1–9.

[23] C. Lin, Analysis of three-dimensional heat and fluid flow induced by piezoelectric fan, International Journal of Heat and Mass Transfer 55 (2012) 3043–3053.

[24] M. A. Bidakhvidi, S. Vanlanduit, R. Shirzadeh, D. Vucinic, Experimental and computational analysis of the flow induced by a piezoelectric fan, in: 15th International Symposium on Flow Visualisation, 2012.

[25] A. Agarwal, K. P. Nolan, J. Stafford, N. Jeffers, Visualization of three-dimensional structures shed by an oscillating beam, Journal of Fluids and Structures 70 (2017) 450–463.

[26] J. H. Yoo, J. I. Hong, W. Cao, Piezoelectric ceramic bimorph coupled to thin metal plate as cooling fan for electronic devices, Sensors and Actuators 79 (1) (2000) 8–12.

[27] M. L. Kimber, S. V. Garimella, Measurement and prediction of the cooling characteristics of a generalized vibrating piezoelectric fan, International Journal of Heat and Mass Transfer 52 (19-20) (2009) 4470–4478.

[28] C. Lin, J. Jang, J. Leu, A Study of an Effective Heat-Dissipating Piezoelectric Fan for High Heat Density Devices, Energies 9 (2016) 1–16.

[29] A. Eastman, M. L. Kimber, Aerodynamic damping of sidewall bounded oscillating cantilevers, Journal of Fluids and Structures 51 (2014) 148–160.

[30] L. K. Tan, J. Zhang, X. Tan, Numerical investigation of convective heat transfer on a vertical surface due to resonating cantilever beam, International Journal of Thermal Sciences 80 (2014) 93–107.

[31] S. Liu, R. Huang, W. Sheu, C. Wang, Heat transfer by a piezoelectric fan on a flat surface subject to the influence of horizontal/vertical arrangement, International Journal of Heat and Mass Transfer 52 (2009) 2565–2570.

[32] T. Acikalin, S. M. Wait, S. V. Garimella, A. Raman, Experimental investigation of the thermal performance of piezoelectric fans, Heat Transfer Engineering 25 (1) (2004) 4–14.

[33] S. F. Sufian, Z. M. Fairuz, M. Zubair, M. Z. Abdullah, J. J. Mohamed, Thermal analysis of dual piezoelectric fans for cooling multi-LED packages, Microelectronics Reliability 54 (8) (2014) 1534–1543.

[34] S. F. Sufian, M. Z. Abdullah, J. J. Mohamed, Effect of synchronized piezoelectric fans on microelectronic cooling performance, International Communications in Heat and Mass Transfer 43 (2013) 81–89.

[35] S. F. Sufian, M. Z. Abdullah, M. K. Abdullah, J. J. Mohamed, Effect of side and tip gaps of a piezoelectric fan on microelectronic cooling, IEEE Transactions on Components, Packaging and Manufacturing Technology 3 (9) (2013) 1545–1553.

[36] M. L. Kimber, S. V. Garimella, A. Raman, Local heat transfer coefficients induced by piezoelectrically actuated vibrating cantilevers, Journal of Heat Transfer 129 (2007) 1168–1176.

[37] M. K. Abdullah, M. Z. Abdullah, M. V. Ramana, C. Y. Khor, K. A. Ahmad, M. A. Mujeebu, Y. Ooi, Z. Mohd Ripin, Numerical and experimental investigations on effect of fan height on the performance of piezoelectric fan in microelectronic cooling, International Communications in Heat and Mass Transfer 36 (1) (2009) 51–58.

[38] A. Eastman, M. L. Kimber, Flow shaping and thrust enhancement of sidewall bounded oscillating cantilevers, International Journal of Heat and Fluid Flow 48 (2014) 35–42.

[39] J. Stafford, N. Jeffers, Aerodynamic performance of a vibrating piezoelectric fan under varied operational conditions, IEEE Transactions on Components, Packaging and Manufacturing Technology (2014) 1–11.

[40] M. L. Kimber, S. V. Garimella, A. Raman, An experimental study of fluidic coupling between multiple piezoelectric fans, in: Thermomechanical Phenomena in Electronic Systems, 2006, pp. 333–340.

[41] M. K. Abdullah, N. C. Ismail, M. Abdul Mujeebu, M. Z. Abdullah, K. A. Ahmad, M. Husaini, M. N. A. Hamid, Optimum tip gap and orientation of multi-piezofan for heat transfer enhancement of finned heat sink in microelectronic cooling, International Journal of Heat and Mass Transfer 55 (21-22) (2012) 5514–5525.

[42] J. M. Gere, S. P. Timoshenko, Mechanics of Materials, 4th Edition, PWS Publishing Company, Boston, 1997.

[43] S. M. Wait, S. Basak, S. V. Garimella, A. Raman, Piezoelectric fans using higher flexural modes for electronics cooling applications, IEEE Transactions on Components and Packaging Technologies 30 (1) (2007) 119–128.

[44] Z. M. Fairuz, S. F. Sufian, M. Z. Abdullah, M. Zubair, M. S. Abdul Aziz, Effect of piezoelectric fan mode shape on the heat transfer characteristics, International Communications in Heat and Mass Transfer 52 (2014) 140–151.

[45] W. Sheu, R. Huang, C. Wang, Influence of bonding glues on the vibration of piezoelectric fans, Sensors and Actuators A: Physical 148 (2008) 115–121.

[46] K. Hao Tseng, M. Mochizuki, K. Mashiko, T. Kosakabe, E. Takenaka, K. Yamamoto, R. Kikutake, Piezo fan for thermal management of electronics, Fujikura Technical Review (2010) 39–43.

[47] T. Acikalin, S. V. Garimella, J. Petroski, A. Raman, Optimal design of miniature piezoelectric fans for cooling light emitting diodes, in: Thermal and Thermomechanical Phenomena in Electronic Systems, 2004, pp. 663–671.

[48] J. Shyu, J. Syu, Plate-fin array cooling using a finger-like piezoelectric fan, Applied Thermal Engineering 62 (2014) 573–580.

[49] H. K. Ma, C. L. Liu, H. C. Su, W. H. Ho, Study of a cooling system with a piezoelectric fan, in: 28th SEMI-THERM Symposium, 2012, pp. 243–248.

[50] L. A. Florio, A. Harnoy, Use of a vibrating plate to enhance natural convection cooling of a discrete heat source in a vertical channel, Applied Thermal Engineering 27 (13) (2007) 2276–2293.

[51] T. M. Jeng, C. H. Liu, Moving-orientation and position effects of the piezoelectric fan on thermal characteristics of the heat sink partially filled in a channel with axial flow, International Journal of Heat and Mass Transfer 85 (2015) 950–964.

[52] C. H. Huang, G. Y. Fan, Determination of relative positions and phase angle of dual piezoelectric fans for maximum heat dissipation of fin surface, International Journal of Heat and Mass Transfer 92 (2016) 523–538.

[53] M. L. Kimber, R. Lonergan, S. V. Garimella, Experimental study of aerodynamic damping in arrays of vibrating cantilevers, Journal of Fluids and Structures 25 (8) (2009) 1334–1347.

[54] M. Choi, S. Y. Lee, Y. H. Kim, On the flow around a vibrating cantilever pair with different phase angles, European Journal of Mechanics B/Fluids 34 (2012) 146–157.

[55] M. Choi, C. Cierpka, Y. H. Kim, Effects of the distance between a vibrating cantilever pair, European Journal of Mechanics B/Fluids 43 (2014) 154–165.

[56] R. R. Schmidt, Local and average transfer coefficients on a vertical surface due to convection from a piezoelectric fan, in: Intersociety Conference on Thermal Phenomena in Electronic Systems, 1994, pp. 41–49.

[57] H. K. Ma, Y. T. Li, C. P. Lin, Study of a dual-sided multiple fans system with a piezoelectric actuator, Journal of Thermal Science 24 (5) (2015) 432–441.

[58] H. K. Ma, H. C. Su, W. F. Luo, Investigation of a piezoelectric fan cooling system with multiple magnetic fans, Sensors and Actuators A: Physical 189 (2013) 356–363.

[59] S. F. Sufian, M. Z. Abdullah, Heat transfer enhancement of LEDs with a combination of piezoelectric fans and a heat sink, Microelectronics Reliability 68 (2017) 39–50.

[60] J. Petroski, M. Arik, M. Gursoy, Optimization of piezoelectric oscillating fan-cooled heat sinks for electronics cooling, IEEE Transactions on Components and Packaging Technologies 33 (1) (2010) 25–31.

[61] A. Almoli, A. Thompson, N. Kapur, J. Summers, H. Thompson, G. Hannah, Computational fluid dynamic investigation of liquid rack cooling in data centres, Applied Energy 89 (1) (2012) 150–155.

[62] X. Jiang, C.-H. Lai, Numerical Techniques for Direct and Large-Eddy Simulations, Taylor and Francis, New York, 2009.

[63] R. Peyret, T. D. Taylor, Computation Methods for Fluid Flow, Springer-Verlag Inc., New York, 1983.

[64] M. K. Abdullah, M. Z. Abdullah, S. F. Wong, C. Y. Khor, Y. Ooi, K. A. Ahmad, Z. M. Ripin, M. A. Mujeebu, Effect of piezoelectric fan height on flow and heat transfer for electronics cooling applications, in: 10th International Conference on Electronic Materials and Packaging, 2008, pp. 165–170.

[65] F. Menter, Zonal Two Equation k-w Turbulence Models for Aerodynamic Flows, in: 24th Fluid Dynamics Conference, 1993, pp. 1–21.

[66] D. C. Wilcox, Formulation of the k-w Turbulence Model Revisited, AIAA Journal 46 (11) (2008) 2823–2838.

[67] B. E. Launder, D. B. Spalding, The Numerical Computation of Turbulent Flows, Computer Methods in Applied Mechanics and Engineering 3 (2) (1974) 269–289.

[68] V. Yakhot, S. A. Orszag, S. Thangam, T. B. Gatski, C. G. Speziale, Development of turbulence models for shear flows by a double expansion technique, Physics of Fluids A: Fluid Dynamics 4 (7) (1992) 1510–1520.

[69] T. Acikalin, A. Raman, S. V. Garimella, Two-dimensional streaming flows induced by resonating, thin beams, The Journal of the Acoustical Society of America 114 (4) (2003) 1785–1795.

[70] DeltaElectrionics, Delta Electronics DC Fan Datasheet. Model: FFB0412SHN (2005).

[71] F. Zenger, S. Münsterjohann, S. Becker, Efficient and Noise Reduced Design of Axial Fans Considering Psychoacoustic Evaluation Criteria, Applied Mechanics and Materials 856 (2017) 181–187.

[72] IEA, More Data, Less Energy: Making Network Standby More Efficient in Billions of Connected Devices (2014).

[73] British Petroleum, BP Statistical Review of World Energy 2017 (2017).

[74] USEPA, Inventory of U.S. Greenhouse Gas Emissions and Sinks: 1990-2015 (2017).

[75] D. Arent, J. Pless, T. Mai, R. Wiser, M. Hand, S. Baldwin, G. Heath, J. Macknick, M. Bazilian, A. Schlosser, P. Denholm, Implications of high renewable electricity penetration in the U.S. for water use, greenhouse gas emissions, land-use, and materials supply, Applied Energy 123 (2014) 368–377.